Sox2 deficiency causes neurodegeneration and impaired neurogenesis in the adult mouse brain

Anna L. M. Ferri[1], Maurizio Cavallaro[1], Daniela Braida[2], Antonello Di Cristofano[3], Annalisa Canta[1], Annamaria Vezzani[4], Sergio Ottolenghi[1], Pier Paolo Pandolfi[3], Mariaelvina Sala[2], Silvia DeBiasi[5] and Silvia K. Nicolis[1,*]

[1]Department of Biotechnology and Biosciences, University of Milano-Bicocca, Piazza della Scienza 2, 20126 Milano, Italy
[2]Department of Pharmacology, Chemotherapy and Medical Toxicology, University of Milano, via Vanvitelli 32, 20129 Milano, Italy
[3]Cancer Biology and Genetics Program, and Department of Pathology, Memorial Sloan-Kettering Cancer Center, 1275 York Avenue, Box 110, New York, NY 10021, USA
[4]Department of Neuroscience, 'Mario Negri' Institute of Pharmacological Research, via Eritrea 62, 20157 Milano, Italy
[5]Department of Biomolecular Sciences and Biotechnology, University of Milano, via Celoria 26, 20133 Milano, Italy
*Author for correspondence (e-mail: silvia.nicolis@unimib.it)

Accepted 2 April 2004

Development 131, 3805-3819
Published by The Company of Biologists 2004
doi:10.1242/dev.01204

Summary

In many species, the *Sox2* transcription factor is a marker of the nervous system from the beginning of its development, and we have previously shown that *Sox2* is expressed in embryonic neural stem cells. It is also expressed in, and is essential for, totipotent inner cell mass stem cells and other multipotent cell lineages, and its ablation causes early embryonic lethality. To investigate the role of *Sox2* in the nervous system, we generated different mouse mutant alleles: a null allele (*Sox2*$^{\beta\text{-geo}}$ 'knock-in'), and a regulatory mutant allele (*Sox2*$^{\Delta ENH}$), in which a neural cell-specific enhancer is deleted. *Sox2* is expressed in embryonic early neural precursors of the ventricular zone and, in the adult, in ependyma (a descendant of the ventricular zone). It is also expressed in the vast majority of dividing precursors in the neurogenic regions, and in a small proportion of differentiated neurones, particularly in the thalamus, striatum and septum. Compound *Sox2*$^{\beta\text{-geo}/\Delta ENH}$ heterozygotes show important cerebral malformations, with parenchymal loss and ventricle enlargement, and L-dopa-rescuable circling behaviour and epilepsy. We observed striking abnormalities in neurones; degeneration and cytoplasmic protein aggregates, a feature common to diverse human neurodegenerative diseases, are observed in thalamus, striatum and septum. Furthermore, ependymal cells show ciliary loss and pathological lipid inclusions. Finally, precursor cell proliferation and the generation of new neurones in adult neurogenic regions are greatly decreased, and GFAP/nestin-positive hippocampal cells, which include the earliest neurogenic precursors, are strikingly diminished. These findings highlight a crucial and unexpected role for *Sox2* in the maintenance of neurones in selected brain areas, and suggest a contribution of neural cell proliferative defects to the pathological phenotype.

Supplemental data available online

Key words: Neural stem cells, Nervous system, Mouse, Sox2, Transcription factors, Neurogenesis, Hippocampal precursors, Neurodegeneration, Neuronal inclusions

Introduction

Sox (Sry-related HMG box) (Gubbay et al., 1990) genes encode transcription factors regulating crucial developmental decisions in different systems, such as early gonad, crystallin, chondrocytes and glia (Kamachi et al., 2000). These genes are also involved in hereditary diseases in man (Kamachi et al., 2000). *Sox2* is expressed in, and is essential for, totipotent inner cell mass stem cells and other early multipotent cell lineages, and its ablation causes early embryonic lethality (Avilion et al., 2003). In many different species, *Sox2* is a marker of the nervous system from the beginning of its development (Uwanogho et al., 1995; Wood and Episkopou, 1999; Kishi et al., 2000; Kamachi et al., 2000; Avilion et al., 2003); an important role in early neural development is further suggested by experiments in chick and *Xenopus* (Kamachi et al., 2000; Kishi et al., 2000). We previously showed that mouse *Sox2* is expressed in embryonic neural stem cells (Zappone et al., 2000). This observation, together with the crucial role of *Sox2* in early embryonic stem cells (Avilion et al., 2003), suggests that *Sox2* function may be related to important aspects of multipotent cell biology.

To investigate the role of *Sox2* in the nervous system, we generated different mouse mutant alleles: a null allele (*Sox2*$^{\beta\text{-geo}}$ 'knock-in') (Zappone et al., 2000; Avilion et al., 2003), and a regulatory mutant allele (*Sox2*$^{\Delta ENH}$), in which a neural cell-specific enhancer (Zappone et al., 2000) is deleted. Compound *Sox2*$^{\beta\text{-geo}/\Delta ENH}$ heterozygotes are born with important cerebral malformations and neural cell pathology. In addition to proliferative defects of adult stem/progenitor cells, our results unexpectedly reveal a crucial role for *Sox2* in neuronal maintenance in selected brain areas.

Materials and methods

Sox2 gene targeting

The generation of the *Sox2*$^{\beta\text{-geo}}$ null allele has been described (Zappone et al., 2000; Avilion et al., 2003). To generate the regulatory mutation *Sox2*$^{\Delta\text{ENHneo}}$, genomic *Sal*I-*Xho*I and *Hin*dIII-*Xho*I fragments (Zappone et al., 2002) were cloned upstream (in the *Sal*I site) and downstream (in the *Eco*RI site), respectively, to the 'floxed' PGKneo cassette of the ploxPNT vector (a derivative of the pPNT vector in which loxP sites have been added to flank the PGKneo cassette), via appropriate linkers. Vectors were linearized using a unique *Kpn*I site. This targeting construct was amplified at low-copy number in a CMB^{-} *E. coli* strain. Gene targeting was carried out in CJ7 ES cells, as described previously (Zappone et al., 2000), using both positive (G418) and negative (Gancyclovir) selection. Chimaeras were bred to C57BL/6J females to generate F1 heterozygous animals carrying each of the mutant alleles; these were then bred to obtain the compound genotypes. Further breeding was done on the same 129Sv/C57Bl/6J background, by breeding of F1, F2, etc., animals.

β-Geo expression in tissues

X-gal staining was performed as described (Zappone et al., 2000). Fresh-frozen embryos or dissected brains were sectioned at 20-40 μm, air dried, postfixed for 30 minutes in 1% glutaraldehyde in PBS, washed in PBS and stained according to Zappone et al. (Zappone et al., 2000) for 2-4 hours. Sections were then dehydrated through an ethanol series and mounted.

In vitro neurosphere cultures, immunocytochemistry and RT-PCR

Neurosphere cultures were grown in vitro from adult brain lateral ventricles in the presence of G418 for 5-12 passages (about 5-12 weeks), as previously described (Zappone et al., 2000). Individual G418-resistant neurospheres were picked from low-density cultures (to ensure clonal origin), dissociated to single cells, and allowed to grow secondary neurospheres (in G418). Individual neurospheres were again picked, briefly expanded as clonal cultures, allowed to differentiate, then probed with antibodies against β-tubulin 3 (neurones) (BABCO mouse monoclonal, 1:500) and GFAP (astroglia) (Diasorin, rabbit polyclonal, 1:5), or GalC (oligodendroglia) (Chemicon mouse monoclonal, 1:100), followed by detection with FITC or TRITC-conjugated Chemicon secondary antibodies (1:100). For X-gal staining, neurospheres were fixed (Zappone et al., 2000) for 10 minutes and stained for 2 hours.

RT-PCR for *Sox2* (and HPRT control) was performed according to Zappone et al. (Zappone et al., 2000), on DNAse-treated total RNA. Samples obtained after 20 cycles were analyzed by Southern blotting with radioactive probes to obtain a quantitative estimate in the exponential phase of amplification. Images were recorded with a Typhoon 8600 (Molecular Dynamics-Amersham Biosciences) apparatus and analyzed with ImageQuant (Molecular Dynamics) software.

Histology, immunohistochemistry and electron microscopy

For morphological/histological adult brain studies, animals were perfused with 4% paraformaldehyde (PFA) in PBS. Brains were dissected, postfixed overnight in the same fixative, cryoprotected in 30% sucrose, frozen and sectioned at 40 μm. Sections were stained with thionine, quickly dehydrated through an ethanol series and mounted. Analysis (coronal sections) was performed by complete coronal sectioning of 10 mutant (8 *Sox2*$^{\beta\text{-geo}/\Delta\text{ENHneo}}$ and 2 *Sox2*$^{\beta\text{-geo}/\Delta\text{ENH}\Delta\text{neo}}$) and four wild-type littermates brains. The abnormalities reported were consistently observed in all mutants. For comparisons at E14.5, a total of six mutant and four wild-type embryos were analyzed. The same analyses were carried out on *Sox2*$^{\beta\text{-geo}/+}$ heterozygotes and on *Sox2*$^{\Delta\text{ENH}/\Delta\text{ENH}}$ homozygotes, and no significant difference with respect to wild type was observed, except for a mild ventricle enlargement in the occasional *Sox2*$^{\beta\text{-geo}/+}$ mouse.

For immunohistochemistry of intraneuronal aggregates in adult brain, mice (6-months old) were perfused with 4% PFA in 0.1 M phosphate buffer (PB; pH 7.4), brains were postfixed for 12 hours to 2 days, dehydrated in ethanols and embedded in paraffin wax. Dewaxed and rehydrated 10 μm sections were blocked with 1% BSA in PBS for 30 minutes, incubated for 48 hours at 4°C in primary antibodies, followed by the appropriate biotinylated secondary antibodies and developed with a standard Vector ABC kit. Four mutant and four wild-type littermates brains were analyzed; all mutants (and no wild-type) showed the alterations described. Primary antibodies were: SMI 32 (non-phosphorylated neurofilaments) and SMI 31 (phosphorylated neurofilaments) (Sterberger monoclonals, both 1:1000), anti-ubiquitin (Chemicon monoclonal, 1:1000). Immunolabelled sections were lightly counterstained with thionine.

For histology on semithin sections and electron microscopy, mice were perfused with 2.5% glutaraldehyde and 0.5% paraformaldehyde, and brains were postfixed in the same fixative overnight. Coronal vibratome sections (80 μm) were osmicated and flat-embedded in Epon-Spurr. Semithin (1 μm) sections were stained with Toluidine Blue for light microscopy, and adjacent thin sections collected on grids were counterstained with uranyl acetate and lead citrate and viewed in a Jeol electron microscope.

For SOX2 immunodetection, paraffin sections were prepared as above and pre-treated for antigen unmasking by bringing to the boil (in a microwave oven) in citrate buffer, then incubated with a rabbit polyclonal anti-SOX2 antibody (Chemicon, 1:500) for 24-48 hours at room temperature. Incubation with a biotinylated secondary antibody (VECTOR, 1:200) was then performed, followed by revelation with the VECTASTAIN ABC system (VECTOR) using DAB as the chromogen. For SOX2/BrdU double immunofluorescence, 30 μm cryosections (prepared as above, morphological studies) were microwaved for antigen unmasking (see above), then pre-treated for BrdU immunodetection as described below, and then incubated with a mixture of rabbit anti-SOX2 (see above) and rat anti-BrdU (see below) primary antibodies (24-36 hours), followed by fluorescent Rhodamine-X anti-rat (see below) and FITC anti-rabbit (Jackson, 1:200) secondary antibodies. For SOX2/GFAP and SOX2/PSA-NCAM double immunofluorescence, cryosections (as for SOX2/BrdU) were pre-treated for antigen unmasking as above, and incubated with a mixture of rabbit anti-SOX2 and either mouse monoclonal anti-GFAP antibody (Boehringer, 1:200) or mouse anti-PSA-NCAM monoclonal antibody (AbCys S.A., Paris, 1:800). For SOX2/GFAP detection, this was followed by FITC anti-rabbit and Rhodamine-X anti-mouse (both Jackson, 1:200) secondary antibodies. For SOX2/PSA-NCAM detection, secondary antibodies were Rhodamine-X anti-rabbit (Jackson, 1:200) and Cy2 anti-mouse IgM (Jackson, 1:200).

For nestin and nestin/GFAP double immunofluorescence, cryosections (30 μm) were prepared as above (no unmasking) and incubated with an anti-nestin antiserum (nestin 130, a gift from R. McKay, 1:50) and (for the double immunofluorescence) a monoclonal anti-GFAP antibody (Boehringer, 1:200). For the single GFAP staining using DAB reaction, the same anti-GFAP antibody was used, at a dilution of 1:1000.

Appropriate controls for all antibodies used ruled out non-specific reactions by secondary antibodies, or cross-reactions between antibodies used simultaneously. SOX2 immunoreactivity was quantitated in DAB-stained sections by densitometry of equivalent areas of the periventricular region (embryo); for adult sections, the average staining of the populations of *Sox2*-positive cells was obtained by individually scanning all visible cells in a field and subtracting the average background staining. Densitometric analysis was carried out using ImageQuant (Molecular Dynamics) software.

In situ hybridization

A *Sox2* probe was transcribed from an *Acc*I-*Xba*I 750 nucleotide fragment (Avilion et al., 2003), and hybridized to 80 μm vibratome sections essentially as described by Wilkinson (Wilkinson, 1998). Briefly, sections were treated in 2% H_2O_2 in PBT (0.1% Triton X-100 in PBS) for 1 hour, washed in PBT, treated with proteinase K (10 μg/ml in PBT) for 8 minutes, incubated with 2 mg/ml glycine in PBS for 10 minutes, prehybridized and hybridized at 60°C overnight with 1 μg/ml probe in 50% formamide, 5×SSC (pH 4.5), 1% SDS and 50 μg/ml yeast RNA. Sections were then successively washed with 50% formamide, 5×SSC (pH 4.5), 1% SDS (for 1 hour at 60°C), 0.5 M NaCl, 10 mM TrisCl (pH 7.5), 0.1% Tween-20 (for 1 hour at room temperature), and then with 50% formamide, 2×SSC (pH 4.5) (for 1 hour at room temperature). Washing was followed by preincubation in TBST [0.5 M NaCl, 20 mM Tris (pH 7.5), 0.1% Tween-20] with 10% normal goat serum (NGS) (for 90 minutes at room temperature), and incubation with anti-DIG antibody (Boehringer, 1:2000) in TBST with 1% NGS overnight at 4°C. This was followed by several washes in TBST, and then in NTMT [100 mM NaCl, 100 mM TrisCl (pH 9.5), 50 mM $MgCl_2$, 0.1% Tween-20], and incubation in BM-purple DIG substrate (SIGMA). Sections were then postfixed briefly and mounted in 80% glycerol in PBS.

Quantitation of the hybridization signal was carried out on equivalent areas of the periventricular region by densitometric scanning using ImageQuant software.

BrdU labelling and immunohistochemistry

BrdU was administered to adult mice (75 μg/g intraperitoneally) with a daily injection for 6 days (or 9 days for BrdU/calbindin double labelling, see below), and it was also supplied in the drinking water at 1 mg/ml. Mice were perfused on the seventh day (or twelfth day for BrdU/calbindin double labelling) with 4% paraformaldehyde and treated for cryosectioning as above. For a total count of BrdU-positive cells, 10-20 μm sections were cut, air dried, and treated with 50% formamide, 50% 2×SSC at 65°C for 1 hour. This was followed by washes in 2×SSC at room temperature, denaturation with 2N HCl in H_2O at 37°C for 1 hour, neutralization with 0.1 M borate buffer (pH 8.5) for 10 minutes and treatment with 0.6% H_2O_2 in PBS for 10 minutes at room temperature. Sections were then blocked in 1% BSA in PBS for 1 hour at room temperature, and probed with a SIGMA anti-BrdU mouse monoclonal antibody (1:150, in 0.1% BSA in PBS) overnight at 4°C. Secondary fluorescent or biotinylated antibodies were subsequently used, and sections were dehydrated and mounted. BrdU-positive nuclei surrounding the lateral ventricles, or in the germinative layer of the dentate gyrus, were counted on one out of every four coronal sections along the entire extension of the forebrain.

For neurogenesis studies by BrdU/calbindin double labelling, 40 μm floating cryosections were cut, treated as above for BrdU immunostaining (except for omission of the formamide/SSC pre-treatment), and incubated overnight at room temperature with rat anti-BrdU (Harlan, 1:500) and rabbit anti-calbindin (SWANT, 1:200) antibodies, followed by rhodamine-X fluorescent anti-rat (Jackson, 1:200), biotinylated anti-rabbit (VECTOR, 1:200 followed by FITC-streptavidin, Jackson, 1:200) secondary antibodies. For quantification, BrdU/calbindin double-positive and BrdU single-positive cells were counted on one out of every three coronal sections throughout the length of the hippocampus. For lateral ventricle BrdU/β-tubulin double immunofluorescence studies, the method described by Capela and Temple (Capela and Temple, 2002) was used. Briefly, periventricular cells were dissociated and allowed to adhere to polylysine-coated plastic chambered slides for 2-3 hours, then fixed with 4% paraformaldehyde, pre-treated for BrdU immunostaining (as above) and reacted with a mixture of rat anti-BrdU and rabbit polyclonal anti-β-tubulin antibodies. A minimum of 500 cells (corresponding to an average of 200 BrdU-positive cells for the wild type) were counted for each mouse.

Behavioral tests

Animals were individually housed in laboratory cages, with a 12-hour light-dark cycle, with free access to food and water throughout the study.

Spontaneous motor activity

Mice from each genotype were placed in an activity cage (Ugo Basile, Varese, Italy) as previously described (Braida et al., 2000). Cumulative horizontal counts (measuring horizontal motility) were recorded for 30 minutes.

Circling behavior

Rotations of each animal were recorded by an observer, blind of treatments, during motor activity test. Cumulative turns were evaluated for 30 minutes, by counting for 1 minute every 5 minutes. Only complete (360°) left or right rotations were counted for quantification of circling behavior. All experiments were performed during the light period between 9 am and 1 pm. Each animal was subjected to all forms of treatments in a random order with at least one week elapsing between experiments.

Evaluation of EEG activity

Mice were surgically implanted under deep Equithesin anesthesia (1% phenobarbital/4% chloral hydrate, 3 ml/kg, ip, Sigma) with a unilateral bipolar hippocampal electrode and a screw electrode positioned onto the contralateral overlying cortex under stereotaxic guidance, as previously described (Vezzani et al., 2000). The coordinates from bregma for the implantation of the electrodes were (mm): anteroposterior, –1.9; lateral±1.5; horizontal, 1.5 below dura. The electrodes were connected to a multipin socket and secured to the skull with acrylic dental cement. Animals were allowed 3-5 days to recover from surgical procedures before the start of the experiment.

EEG recordings were carried out in freely-moving mice, as previously described (Vezzani et al., 2000), to assess the spontaneous EEG pattern. The EEG recordings were made twice a day (between 9 am and 12 pm, and 4 and 6 pm) continuously for at least 30 minutes. Mice were recorded three times per week for two consecutive weeks. The EEG of each mouse was visually analyzed by two independent investigators who were unaware of the identity of the experimental groups. Particular attention was paid to the occurrence of ictal episodes (high frequency and/or multispike complexes, and/or high voltage synchronized spikes, simultaneously occurring in both leads of recordings) and/or spiking activity (Vezzani et al., 2000).

Results

Generation of an allelic series of *Sox2* mutations

To generate a null *Sox2* mutation we replaced (Zappone et al., 2000; Avilion et al., 2003) the *Sox2* coding region with the β-geo gene, encoding β-galactosidase and G418 resistance ($Sox2^{\beta\text{-geo}}$ 'knock-in'). In addition, we obtained a regulatory mutation ($Sox2^{\Delta ENHneo}$, Fig. 1) by substituting a G418-resistance cassette (PGKneo), flanked by loxP sites, for an upstream *Sox2* neural cell-specific enhancer (Zappone et al., 2000). This enhancer directs expression specifically to the developing forebrain in transgenic mice (Zappone et al., 2000). Deletion of this enhancer by homologous recombination from the endogenous *Sox2* locus was shown to result in significantly decreased (but not abolished) expression of a linked β-geo 'knock-in' reporter (replacing the *Sox2* gene) in the developing brain (particularly telencephalon, but also diencephalon and mesencephalon) after E12.5 (Zappone et al., 2000) (S.D.B. and S.K.N., unpublished). The PGKneo cassette, replacing the enhancer, was subsequently deleted in vivo ($Sox2^{\Delta ENH\Delta neo}$,

Fig. 1) by crossing to Cre-expressing mice (Schwenk et al., 1995), to avoid any potential inhibition by the cassette of linked gene transcription (McDevitt et al., 1997).

The expression of *Sox2*$^{\beta\text{-geo}}$ in CNS and forebrain development

Using the *Sox2*$^{\beta\text{-geo}}$ knock-in allele, we investigated *Sox2* expression. *Sox2*$^{\beta\text{-geo}}$ is highly expressed in embryonic stem (ES) cells (Fig. 2A), as in the blastocyst inner cell mass (Zappone et al., 2000; Avilion et al., 2003). Following gastrulation, expression is seen in neurogenic regions: the neural plate (E7.5, Fig. 2B) and, thereafter, the entire neural tube (E12.5, Fig. 2C). In the differentiating neural tube, expression persists in the proliferating ventricular zone, and is diminished in outer layers, where differentiation takes place (Fig. 2D,E,F). However, in the thalamus, medial-dorsal striatum and septum, significant expression is maintained in differentiating areas during embryogenesis (Fig. 2E,F) and postnatally (Fig. 2I,J,M). Expression is also seen in choroid plexi (Fig. 2G). In the adult, high-level expression is seen in the ependyma (the descendant of the embryonic ventricular zone) throughout the neural tube (Fig. 2H-L, and data not shown) and in the subependyma (Fig. 2K,L). This includes the adult neurogenic region of the lateral ventricle, from where expression extends along the entire rostral migratory stream (RMS) (Fig. 2H), along which dividing precursors migrate to the olfactory bulb. The germinative layer of the hippocampus dentate gyrus, another site of adult neurogenesis (McKay, 1997; Gage, 2000), also expresses *Sox2*$^{\beta\text{-geo}}$, at lower levels (Fig. 2N).

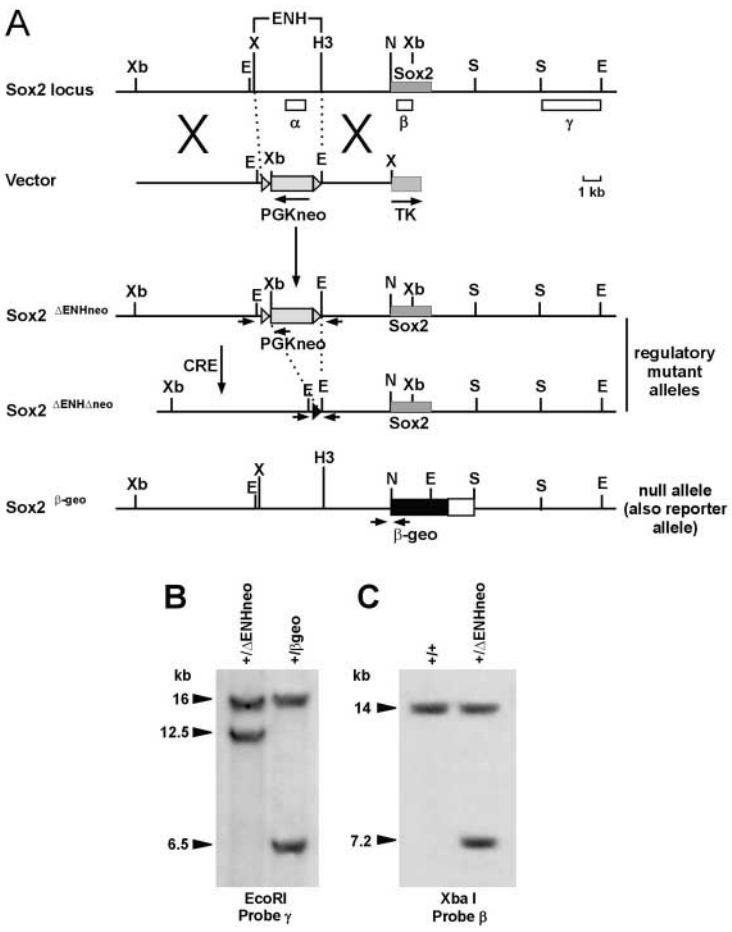

Fig. 1. Generation of an allelic series of *Sox2* mutations by gene targeting. (A) A schematic diagram of the *Sox2* locus (top) and targeting vector used to generate the *Sox2*$^{\Delta\text{ENHneo}}$ regulatory mutant allele (middle) in ES cells. From this mutant allele, *Sox2*$^{\Delta\text{ENH}\Delta\text{neo}}$ is obtained by in vivo Cre-mediated excision of the neo cassette. The *Sox2*$^{\beta\text{-geo}}$ null/reporter allele (bottom) was previously described (Zappone et al., 2000). The PGKneo and PGKTK cassettes are derived from the pPNT vector. ENH is the DNA region containing the brain enhancer described by Zappone et al. (Zappone et al., 2000); α,β and γ are probes used for Southern analysis [for details of α and γ see Zappone et al. (Zappone et al., 2000)], β is an *Acc*I-*Xba*I 750 nucleotide fragment within the *Sox2* coding region; E, *Eco*RI; S, *Sal*I; N, *Not*I; H3, *Hin*dIII; X, *Xho*I; Xb, *Xba*I. Grey triangles indicate loxP sites; arrows indicate PCR primers used for verifying PGKneo deletion. (B,C) Southern analysis of *Eco*RI (B) and *Xba*I (C) digests of ES cell clones. In B, probe γ detects a 16 kb band from the wild-type allele, a 12.5 kb band from the *Sox2*$^{\Delta\text{ENHneo}}$ allele, and a 6.5 kb band from the *Sox2*$^{\beta\text{-geo}}$ allele. In C, probe β detects a 14 kb band from the wild-type allele, and a 7.2 kb band from the *Sox2*$^{\Delta\text{ENHneo}}$ allele. Cre-mediated in vivo deletion of the PGKneo cassette from the *Sox2*$^{\Delta\text{ENHneo}}$ allele was diagnosed by PCR (see above) and confirmed by Southern analysis with both a neo probe and probe α (not shown).

Sox2 expression in the developing and adult brain

To allow a more precise characterization of *Sox2*-expressing neural cell types, particularly in the adult brain, we performed immunohistochemistry experiments with anti-SOX2 antibodies (Figs 3, 4). In the developing brain, SOX2 is found in the ventricular zone (see Fig. S1 at http://dev.biologists.org/supplemental/, and data not shown), matching the distribution seen both by X-gal staining (Fig. 2D-F) and by β-galactosidase immunohistochemistry (data not shown). In late embryogenesis, both parenchymal and ventricular zone expression are observed, as previously seen with X-gal staining (not shown).

In the adult brain, SOX2 is expressed both in sparse cells within differentiated regions (cortex, striatum, thalamus) (Fig. 3E-I) and within neurogenic regions (periventricular ependyma and subependyma, hippocampus) (Fig. 3A-C, DAB staining; Fig. 4). In particular, within differentiated regions, SOX2 is expressed in at least some characteristic pyramidal cells in the cerebral cortex (Fig. 3E,F), in differentiated neurones in the striatum (Fig. 3G) and, abundantly, in the thalamus (particularly in the periventricular nuclei) (Fig. 3H). Positive cells are occasionally detected in the corpus callosum (Fig. 3I) and thus are likely to represent rare SOX2-positive glial cells, as is also suggested by the GFAP positivity (not shown).

In the ventricular zone, ependymal cells and choroid plexi are strongly positive (Fig. 3C,D). Furthermore, the lateral ventricle adjacent to the rostral migratory stream, and the stream itself, include numerous cells strongly positive for SOX2 expression (Fig. 3A,B), again matching β-galactosidase distribution (Fig. 2H,K,L). In the hippocampus dentate gyrus, many neurones are weakly positive (using DAB staining), whereas a minority of the cells show stronger expression (data not shown; see also below, Fig. 4).

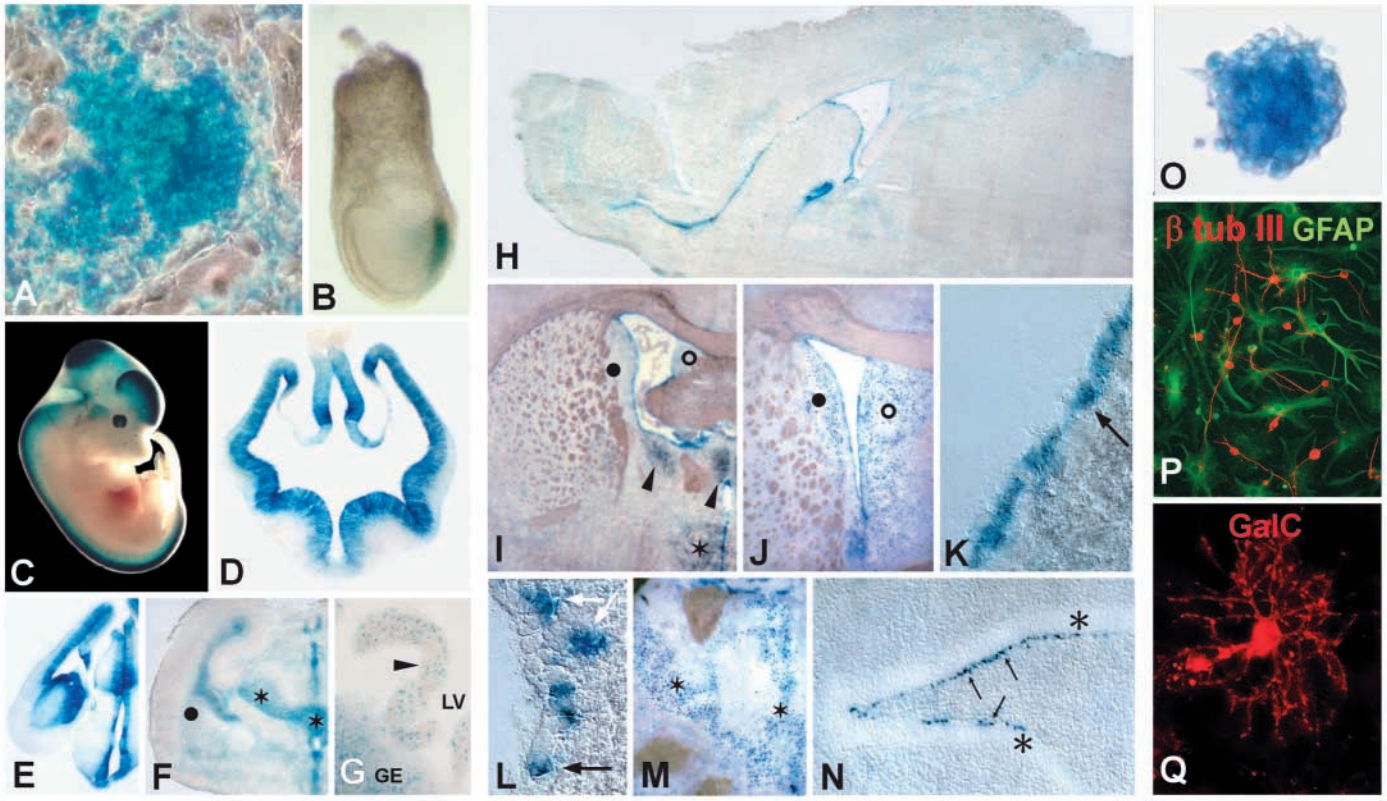

Fig. 2. *Sox2*$^{\beta\text{-geo}}$ expression (X-gal staining, blue) in neural and forebrain development and in adult neural stem cells from *Sox2*$^{\beta\text{-geo/+}}$ mice. (A) Undifferentiated ES cells; (B) E7.5 neural plate stage. Right, anterior; left, posterior. A few blue cells are also visible at the base of the allantois, where the first appearance of primordial germ cells has been described. (C) E12.5 embryo; (D-G) coronal sections of forebrain at E11.5 (D), E12.5 (E) and E17.5 (F,G). In F, asterisks indicate developing thalamic nuclei, basolateral (more external) and centromedian and paraventricular (closer to the midline); black circle indicates the striatum. In G, the black arrowhead indicates the choroid plexus. GE, ganglionic eminence; LV, lateral ventricle. (H-Q) Adult brain. (H) Sagittal section with anterior to the left and posterior to the right. Brief X-gal reaction development. Note the intensely stained ventricle lining and rostral migratory stream. (I,J) Coronal sections (I is more posterior than J) after a prolonged X-gal reaction development. Asterisk and black arrowheads, thalamic nuclei; black circle, dorsal striatum; white circle, septum. (K,L) Interference contrast microscope view of lateral ventricle wall showing details from a section corresponding to that shown in J. Black arrow, ependymal staining; white arrows, subependymal staining. (M) Thalamic region detail, at a level slightly posterior to that shown in I (and corresponding to that shown in F; see F, I and J for symbols). (N) Hippocampus dentate gyrus (long X-gal reaction development). Arrows indicate the germinative layer; asterisks indicate the granule cell layer. (O) Neurospheres, the progeny of stem cells, grown in vitro from adult brain lateral ventricles in the presence of G418 for 5-12 passages (about 5-12 weeks) express *lacZ* in most cells. (P,Q) Cells obtained by differentiation of the clonal progeny of a single G418-resistant (i.e. *Sox2* expressing) cell were probed with antibodies against (P) β-tubulin III (neurones; red) and GFAP (astroglia; green), or (Q**)** GalC (oligodendroglia).

To better characterize the Sox2-expressing cells in the neurogenic regions, double-immunofluorescence experiments were performed. Among neural cells, only stem cells and their early descendants (such as precursors, transit amplifying progenitors and neuroblasts) divide in the adult brain (Temple and Alvarez-Buylla, 1999). We thus labelled proliferating cells by BrdU administration, and investigated whether BrdU-positive cells express SOX2. Most, if not all, BrdU-positive cells in the neurogenic region of the lateral ventricle are also SOX2 positive (Fig. 4A,B, and data not shown). Notably, some of the double BrdU/SOX2-positive cells are found within subependymal cell clusters, as is expected for stem cells or their immediate progeny (Doetsch et al., 1999; Capela and Temple, 2002), whereas the overlying ependyma is BrdU negative (Fig. 4A,B). In addition, many positive cells are also visible in the rostral migratory stream (Fig. 4A).

Neural stem cells have been proposed to be part of a GFAP-positive 'glial' population residing in the subependymal region (Doetsch et al., 1999; Doetsch, 2003). Several cells within the subependyma are labelled with both SOX2 and GFAP antibodies (Fig. 4C,D), and might represent early neural stem cell/precursor cell types. In addition, strongly GFAP-positive cells ensheath newly born (Doetsch et al., 1997; Doetsch et al., 1999; Capela and Temple, 2002) neuroblasts migrating anteriorly along the ventricle to form the rostral migratory stream; these cells appear as 'empty' GFAP-negative areas. Several of these GFAP-negative cells are also SOX2 positive (Fig. 4), indicating that the SOX2-positive/GFAP-negative population may include migrating neuroblasts. Migrating neuroblasts express PSA-NCAM, a membrane antigen, and the proportion of PSA-NCAM-positive cells progressively and strongly increases from posterior to anterior along the migratory route (Doetsch et al., 1997). Strongly SOX2-positive cells were in general PSA-NCAM weakly positive or negative;

however, weakly SOX2-positive cells often showed greater expression of PSA-NCAM (see Fig. S3 at http://dev.biologists.org/supplemental/). At more anterior levels, few if any SOX2/PSA-NCAM double-positive cells were seen.

Thus, SOX2 appears to be expressed in most proliferating neural precursors. The observation of rare GFAP/SOX2-positive cells in the periventricular neurogenic region, together with the expression of SOX2 in essentially all of the BrdU-positive cells in the subventricular zone, suggests that SOX2/GFAP-positive cells may include GFAP-positive neural stem cells.

In the second adult neurogenic region, the hippocampus, SOX2 is expressed along the entire dentate gyrus (Fig. 4E), similar to as observed with *Sox2*$^{\beta\text{-geo}}$ (Fig. 2N). However, prominent expression is detected only in a minority of the cells, at the base of the granule cell layer (Fig. 4F-H). To better characterize these cells, we labelled proliferating precursors with BrdU. Most BrdU-positive cells were located at the base of the granule cell layer, and the large majority of these cells were also strongly SOX2 positive (Fig. 4G). BrdU-positive cells located more deeply inside the granule cell layer showed a much lower level of SOX2 expression, or no expression at all (not shown). As in the subventricular region, 'stem cells' in the hippocampus have been reported to be part of a GFAP-positive population (Seri et al., 2001; Fukuda et al., 2003). Double SOX2/GFAP-positive cells are detected almost exclusively at the base of the granule cell layer, in a location corresponding to that of double SOX2/BrdU-positive cells, with GFAP-labelled processes characteristically extending radially into the granule cell layer (Fig. 4H).

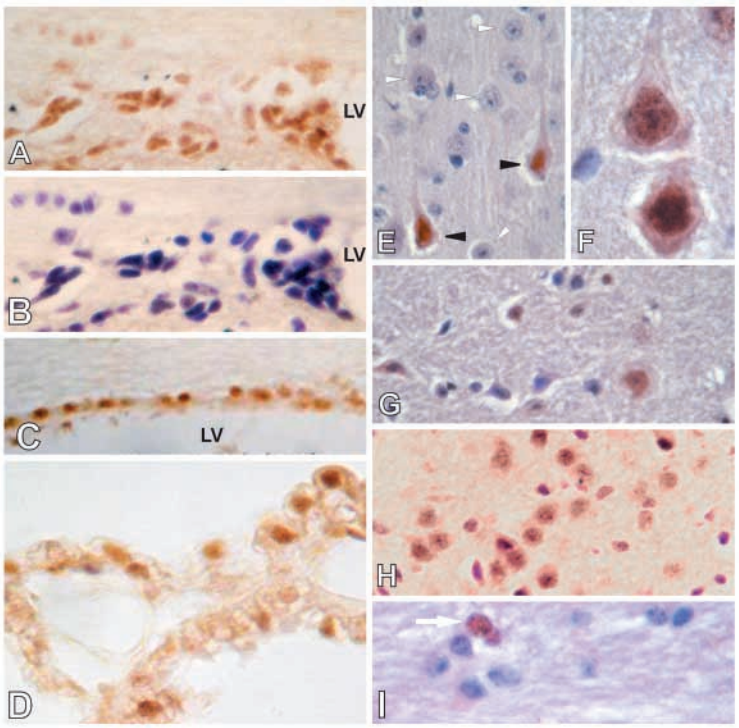

Fig. 3. *Sox2*-expressing cells in the adult brain (DAB staining). (A,B) Origin of the rostral migratory stream in the top corner of the lateral ventricle. Both SOX2 immunostaining (brown) and Haematoxylin counterstaining (blue) of the same section identify a nuclear location. (C) SOX2 immunostaining of lateral ventricle ependyma. (D) SOX2 expression in choroid plexi. (E,F) SOX2-positive (brown) pyramidal cells in cortex (black arrowheads in E), with haematoxylin counterstaining (blue); F shows a higher magnification image. White arrowheads in E indicate SOX2-negative cells. (G) SOX2-positive cells in the striatum (brown). (H) Abundant SOX2-positive cells in the thalamus (brown) with light haematoxylin counterstaining (blue). (I) Occasional SOX2-positive cell (arrow) observed in the corpus callosum.

Sox2 is expressed in neural stem cells grown in vitro from adult brain

Neural stem cells have been grown in vitro from the neurogenic regions of adult mice (McKay, 1997; Gage, 2000; Temple, 2001). To investigate whether *Sox2*$^{\beta\text{-geo}}$ is expressed in adult neural stem cells, we exploited the ability of the β-geo fusion protein to confer resistance to G418. Neural stem cells from the periventricular region of adult *Sox2*$^{\beta\text{-geo}}$ mice were tested in clonal in vitro assays (Zappone et al., 2000). Cells from these cultures extensively self-renew, forming neurospheres, for at least 12 passages (i.e. about 12 weeks), even in the presence of G418, indicating that neurosphere-forming cells continuously express the *Sox2*$^{\beta\text{-geo}}$ knock-in reporter (Fig. 2O). Moreover, individual G418-resistant neurosphere-forming cells retain multipotency, that is the ability to give rise to progeny able to differentiate into all three main neural lineages, neurones, astroglia and oligodendroglia (Fig. 2O-Q). These results indicate that adult neural stem cells grown in vitro continuously express *Sox2*$^{\beta\text{-geo}}$.

Sox2 deficiency causes reduced viability and neurological defects

Homozygosity for the *Sox2*$^{\beta\text{-geo}}$ null allele results in early embryonic lethality (Avilion et al., 2003). Compound *Sox2*$^{\beta\text{-geo}/\Delta\text{ENH}}$ heterozygotes, irrespective of whether the PGKneo cassette has been retained or not, show severe abnormalities, as described below; the two genotypes will be discussed together.

Sox2 expression was evaluated in compound heterozygotes for the null and the knockdown alleles (*Sox2*$^{\beta\text{-geo}/\Delta\text{ENHneo}}$) by antibody staining, in situ hybridization and RT-PCR on neural precursors, grown in vitro as neurospheres (see Figs S1 and S2 at http://dev.biologists.org/supplemental/; data not shown). As anticipated for a regulatory mutation, Sox2 was still detected in the expected brain regions in compound *Sox2*$^{\beta\text{-geo}/\Delta\text{ENHneo}}$ heterozygotes, but at a reduced level (approximately 25-30% relative to the wild-type genotype). As this level of expression is due only to the *Sox2*$^{\Delta\text{ENH}}$ allele, the transcriptional output of this allele is about half that of a wild-type *Sox2* allele.

Neither simple heterozygotes (*Sox2*$^{\beta\text{-geo}/+}$ or *Sox2*$^{\Delta\text{ENH}/+}$) nor *Sox2*$^{\Delta\text{ENH}/\Delta\text{ENH}}$ homozygotes show the abnormalities described for compound *Sox2*$^{\beta\text{-geo}/\Delta\text{ENHneo}}$ heterozygotes. The fact that *Sox2*$^{\Delta\text{ENH}/\Delta\text{ENH}}$ homozygotes are not affected is consistent with the ~50% reduction of expression of the *Sox2*$^{\Delta\text{ENH}}$ allele, which would give a level of *Sox2* expression in *Sox2*$^{\Delta\text{ENH}/\Delta\text{ENH}}$ homozygotes close to that expected for the *Sox2*$^{\beta\text{-geo}/+}$ null heterozygotes.

The viability of the *Sox2*$^{\Delta\text{ENH}/+}$, *Sox2*$^{\beta\text{-geo}/+}$ and *Sox2*$^{\Delta\text{ENH}/\Delta\text{ENH}}$ genotypes was identical to that of

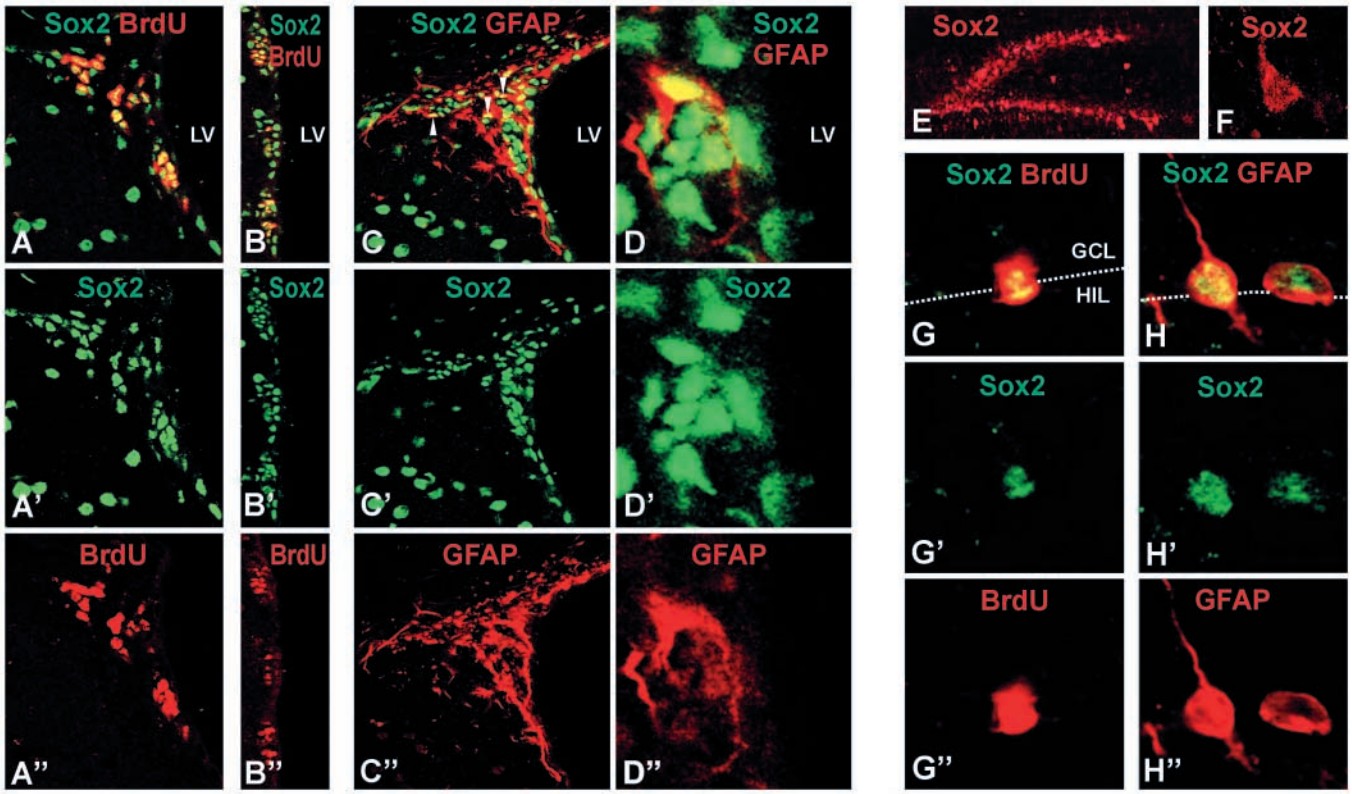

Fig. 4. Double immunofluorescence characterization of *Sox2*-expressing cells in adult neurogenic regions (by confocal microscopy). Coronal sections from mice treated with BrdU for one week. (A-D″) Sections comprising the lateral ventricle were labelled with antibodies against SOX2 (green, A′-D′), BrdU (red, A″,B″) and GFAP (red, C″,D″). Co-expression of SOX2 and BrdU, or SOX2 and GFAP results in yellow staining in merged images (A-D). (A,C) Top corner of lateral ventricle, comprising the origin (top left of each panel) of the rostral migratory stream. In C, white arrowheads indicate some of the SOX2/GFAP double-positive cells in the rostral migratory region. (B) Detail of the ventricle wall, lining the striatum. (D) Magnification of a detail of the ventricle wall, adjacent to the striatum, showing a subependymal SOX2/GFAP double-positive cell [for the morphology of GFAP-positive cells in a similar region, see Doetsch (Doetsch, 2003)]. (E-G**)** Sections comprising the basal portion of the hippocampus dentate gyrus. (E) General view of anti-SOX2-labelled dentate gyrus (red). (F) Magnification of a SOX2-positive cell at the basis of the dentate gyrus. (G,H) SOX2/BrdU (G) and SOX2/GFAP (H) double-positive cells are located in the germinative zone at the basis of the dentate gyrus. (G′,H′) SOX2, green label; (G″) BrdU or (H″) GFAP, red label. (G,H) Yellow indicates double positivity. The position of the cell relative to the germinative cell layer (GCL) is indicated by a dotted white line, which represents the border between the GCL and the hilus (HIL).

the wild type. By contrast, compound *Sox2*$^{\beta\text{-geo}/\Delta\text{ENH}}$ heterozygotes were born in reduced numbers compared with the expected frequency, and their number further declined in postnatal life (Fig. 5A). They showed growth retardation, normally compensated by six weeks of age, and slowed reactivity. When held by their tail, 40% of the mutants retracted their limbs toward their trunk in a dystonic fashion, rather that extending them as did control littermates. This feet-clasping phenotype is observed in several mutants with neurological impairment due to neurodegeneration (Mangiarini et al., 1996; Mantamadiotis et al., 2002; Wang et al., 2002). Forty percent of the mutants showed epileptic spikes in the cortex and hippocampus in electroencephalographic recordings (Fig. 5B). Finally, ‘circling’ behaviour was observed in *Sox2*$^{\beta\text{-geo}/\Delta\text{ENH}}$ mutants at 3-4 weeks of age, or later; this phenotype was transmitted with incomplete penetrance (25%).

In rodents, circling has been linked to striatal neurodegeneration in Huntingtin transgenics (Hodgson et al., 1999) and to drug-induced defects of dopamine supply to the striatum (Kim et al., 2002), indicating the involvement of the basal ganglia-thalamo-cortical circuitry (see Wang et al., 2002). Inadequate dopamine supply is the hallmark of Parkinson’s disease in humans. Administration of L-dopa, a dopamine precursor, causes recovery from motor dysfunction both in Parkinson patients and in mice with drug-induced circling (Kim et al., 2002). Both L-dopa and D1, and particularly D2, dopamine receptor agonists (SKF and quinpirole, respectively) drastically reduced circling in mutant mice (Fig. 5C), and restored horizontal motility (a global measure of ‘general’ horizontal movement, see Materials and methods) to values close to normal (Fig. 5D). Horizontal motility of wild-type animals (that consists of normal movement around the cage, but not circling) did not vary significantly following treatment (Fig. 5D), indicating that the effect of the dopamine receptor agonists was specific for the pathological circling movement.

These findings indicate that a dysfunction in the dopaminergic system is involved in generating circling in the mutants, working through reduced D1 and particularly D2 receptor signalling.

Neurological abnormality is accompanied by brain morphological defects

In adult mutant brains, the cortex is reduced, in particular posteriorly and medially (Fig. 6A,F, sections). In addition, there is progressive anteroposterior reduction of the corpus callosum [that is prematurely interrupted (Fig. 6C) in most mutants, and is completely absent in 15% of the mice), marked decrease of anterior thalamus, dorsal striatum and septum (Fig. 6B-D,I), and lateral and third ventricle enlargement (Fig. 6B-E,I). Reduction of the posterior cerebral cortex is consistently observed already at E14.5 (Fig. 6G,H); of note, no ventricle enlargement is yet present at this stage (Fig. 6G,H), indicating that ventricle enlargement does not, per se, initiate the reduction of the cortical parenchyma. Thalamic-striatal reduction and ventricle enlargement are already developed at E17.5 (not shown) and at birth (Fig. 6I). With the exception of a slight ventricle enlargement in occasional mice, none of these changes is seen in *Sox2*$^{\beta\text{-geo}/+}$ heterozygotes.

Neurodegeneration and intraneuronal aggregates are found in specific regions of mutant brains

To gain insight into the causes of these alterations, we examined the mutant adult brains at the cellular level, in regions and in cell types where *Sox2* is expressed (see Figs 2-4).

In the mutant brain, several neurones show typical features of degeneration (Hodgson et al., 1999; Turmaine et al., 2000; Capsoni et al., 2000; Tanemura et al., 2002), such as a severely shrunken and hyperchromatic cell body, nuclear and cytoplasmic condensation, and irregular, 'scalloped' plasma and nuclear membranes (Fig. 7A-D,L), whereas others exhibit characteristic perinuclear inclusions. Neither abnormality was observed in control littermates. The degenerating cells are located in selected regions, such as striatum, and, particularly, septum and thalamus (centromedian and paraventricular nuclei) (Fig. 7A-D), whereas inclusions are observed in the thalamus, in paraventricular nuclei, and (abundantly) in basolateral and lateral geniculate nuclei (Fig. 7E-L), and (less frequently) in striatum (not shown). Significantly, these regions correspond to those where parenchymal shrinkage is observed (Fig. 6B-E), and match areas of persistent *Sox2* expression in late embryonic and adult stages (Fig. 2F,I,J,M; Fig. 3G,H). Inclusions were rarely detected at birth, were abundant at six months of age, and were extremely abundant in mice aged 18-24 months. Neurodegeneration was not observed at birth, was already apparent at three months, and was abundant (Fig. 7) at six months, with little apparent progression at later stages (we cannot rule out a selective effect, as more severely affected mice may be lost prematurely). In several hereditary and multifactorial neuropathies in man and mouse, inclusions are a hallmark of the disease; they result from aggregation of a variety of proteins, such as neurofilaments, tau protein and alpha-synuclein, and are often ubiquitinated (Taylor et al., 2002; Zoghbi and Botas, 2002). In *Sox2* mutant mice, the perinuclear aggregates contain neurofilaments (Fig. 7J) and, less frequently, ubiquitinated protein (Fig. 7K,L), though not alpha-synuclein (not shown). They are found predominantly in otherwise apparently healthy neurones (Fig. 7E,I-K), but occasional 'hyperchromatic'/degenerating cells can also exhibit them (Fig. 7L).

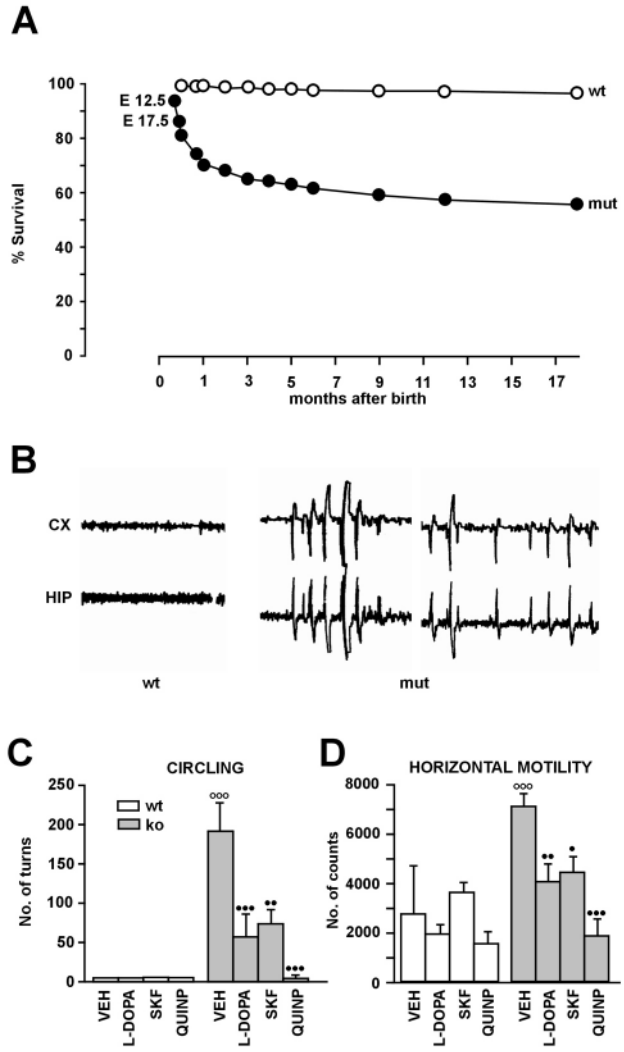

Fig. 5. Reduced viability and neurological abnormalities in *Sox2*$^{\beta\text{-geo}/\Delta ENH}$ mutants. (A) Survival of Sox2$^{\beta\text{-geo}/\Delta ENH}$ compound heterozygotes is decreased (n=50 embryos genotyped; n=510 adults genotyped). (B) Electroencephalography on *Sox2*$^{\beta\text{-geo}/\Delta ENH}$ (mut) and on wild-type (wt) control mice, performed in cortex (cx) and hippocampus (hip). Epileptic-like activity characterized by abnormal synchronized spikes is observed in mutant mice. These spikes appeared in clusters during the recording period and they were intermixed to basal activity similar to that observed in wild-type mice. (C,D) Effect of L-dopa and dopamine receptor agonists on circling and horizontal motility. (C) Decrease in the absolute number of turns (cumulative turns, mean±s.e.m.) and (D) decrease in cumulative horizontal counts (mean±s.e.m.), following administration of L-dopa (50 mg/kg, intraperitoneal injection), SKF 39383 (D1 receptor agonist, 56 mg/kg, subcutaneous) and quinpirole (QUINP; D2 receptor agonist, 3 mg/kg, subcutaneous). The number of turns and of counts were assessed for 30 minutes in wild-type (wt) and *Sox2*$^{\beta\text{-geo}/\Delta ENH(ko)}$ mutant mice. All drugs were given 10 minutes before the tests. A similar percentage decrease of turns was observed for each individual mouse after treatment, irrespective of the absolute basal number of turns. VEH, vehicle (saline). ○○○P<0.001 versus wild-type vehicle-treated group. ●P<0.05, ●●P<0.01 and ●●●P<0.001 versus vehicle-treated mutant group, Tukey's multiple comparison test.

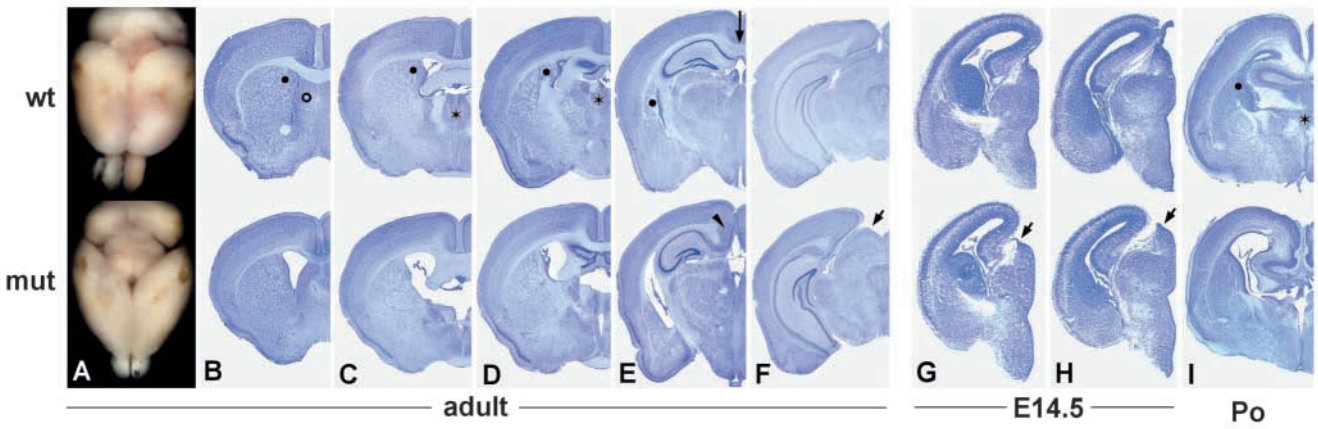

Fig. 6. Morphological alterations of the brain in *Sox2*$^{\beta\text{-geo}/\Delta\text{ENH}}$ mutants. (A) Dorsal view of wild-type (top) and mutant (bottom) brains. The shrinkage of the medial-posterior cortex is particularly visible in this mutant. (B-F) Coronal sections through adult forebrain of a normal (top) and a mutant (bottom) mouse. Sections were matched between normal and mutant brains on the basis of the correspondence of characteristic anatomical landmarks (hippocampus, thalamic nuclei and fibre tracts). Left, anteriormost; right, posteriormost. Asterisk indicates thalamic nuclei (see Fig. 2F). Black circle, dorsal striatum; white circle, septum; arrowhead and arrow in E, corpus callosum. Black arrow in F-H marks the diminished extension of the cortex. (G-I**)** Coronal sections at E14.5 (G,H) and P0 (I) of normal (top) and mutant (bottom) brains. Note, in G and H, the ventricles of the mutant are normal, and the thalamus and striatum sizes are essentially normal, in contrast to the reduced cortex (particularly visible in H).

Ependymal cells abnormalities

Other differentiated cell types in which *Sox2* is expressed is the ependyma and (to a lower extent) the choroid plexi (Figs 2, 3). Thanks to its specialized cilia, the ependyma drives the circulation of the cerebrospinal fluid, produced by the choroid plexi. In the mutant brain the ependyma is abnormal, with large lipidic inclusions and a severe reduction in the number of cilia (Fig. 7M,N). Also, the choroid epithelium develops a large number of infoldings in the basolateral surface, which exchanges fluid and solutes with blood capillaries (Fig. 7O,P).

Impairment of neural cells proliferation and of neurogenesis in adult neurogenic regions

In the ependymal/subependymal region of the lateral ventricles, as well as in the hippocampus dentate gyrus, some neurogenesis is maintained in the adult, through the proliferation and differentiation of neural stem and precursor cells (McKay, 1997; Gage, 2000; Temple, 2001). Adult neural stem cells (a site of *Sox2* expression; Fig. 2O-Q) have been reported to be a subset of ependymal cells themselves (Johansson et al., 1999), or to lie in the subependyma (Doetsch et al., 1999; Capela and Temple, 2002). As *Sox2* is expressed in essentially all dividing progenitors (see above and Fig. 4), we investigated cell proliferation in these regions by BrdU incorporation. In *Sox2*$^{\beta\text{-geo}/\Delta\text{ENH}}$ mutants, the number of BrdU-positive cells was markedly reduced in the hippocampus germinative layer (an ~65% reduction) (Fig. 8A,B) and in the lateral ventricle (an ~55% reduction) (Fig. 8A,B). In the hippocampus, some sparse cells were found in the hilus, where labelling is only rarely seen in the wild type.

As neurogenesis proceeds in the hippocampus, dividing precursors differentiate into granule neurones within the dentate gyrus. We thus evaluated the number of newly generated neurones (i.e. neurones still retaining BrdU positivity) by double-labelling with anti-BrdU and an anti-calbindin antibody, which recognizes differentiated dentate gyrus granule neurones (Kempermann et al., 1997; Gould et al., 1999). As expected from the reduction of BrdU-positive cells, a large decrease in BrdU/calbindin double-positive cells (i.e. newborn neurones) was observed (Fig. 8C,E). Among the few BrdU-positive cells, the proportion of calbindin-positive cells in the mutant mice was reduced (relative to wild type) by more than 50% (Fig. 8E). Thus, the decrease in newly generated (calbindin/BrdU-positive) neurones was much greater than expected simply on the basis of reduced BrdU incorporation. This implies that newly generated precursors from mutant mice have a decreased ability to give rise to fully differentiated (calbindin-positive) neurones.

GFAP-positive radial glia cells in the hippocampus germinative layer generate new neurones in dentate gyrus of adult rats (Seri et al., 2001); in mouse, double GFAP/nestin-positive progenitors share many morphological properties with these cells, and have been identified by BrdU pulse-chase analyses as the earliest progenitors to dentate gyrus adult-born neurones (Doetsch, 2003; Fukuda et al., 2003). In *Sox2*$^{\beta\text{-geo}/\Delta\text{ENH}}$ mutants, nestin-positive cells in the dentate gyrus are greatly decreased (Fig. 9A,C), and GFAP-positive radial glia are also significantly (although less) decreased (Fig. 9B,D). Strikingly, double GFAP/nestin-positive cells are almost absent from the dentate gyrus of mutant mice (Fig. 9E,F). These data suggest that neural stem cells and/or precursors in the adult hippocampal neurogenic region of *Sox2* mutants are depleted.

In the lateral ventricle of adult mice, new neurones arise from precursors located in the subventricular zone, which are variably identified as GFAP-positive (Doetsch et al., 1999) and/or SSEA-positive (Capela and Temple, 2002) cells, or ependymal cells (Johansson et al., 1999). β-Tubulin III is an early marker of neuronal differentiation of these dividing precursors (Capela and Temple, 2002). To allow for easier detection of BrdU and β-tubulin co-localization, we performed double immunofluorescence experiments on dissociated periventricular cells (as reported in Capela and Temple, 2002) (Fig. 8D,F). Double β-tubulin/BrdU-labelled

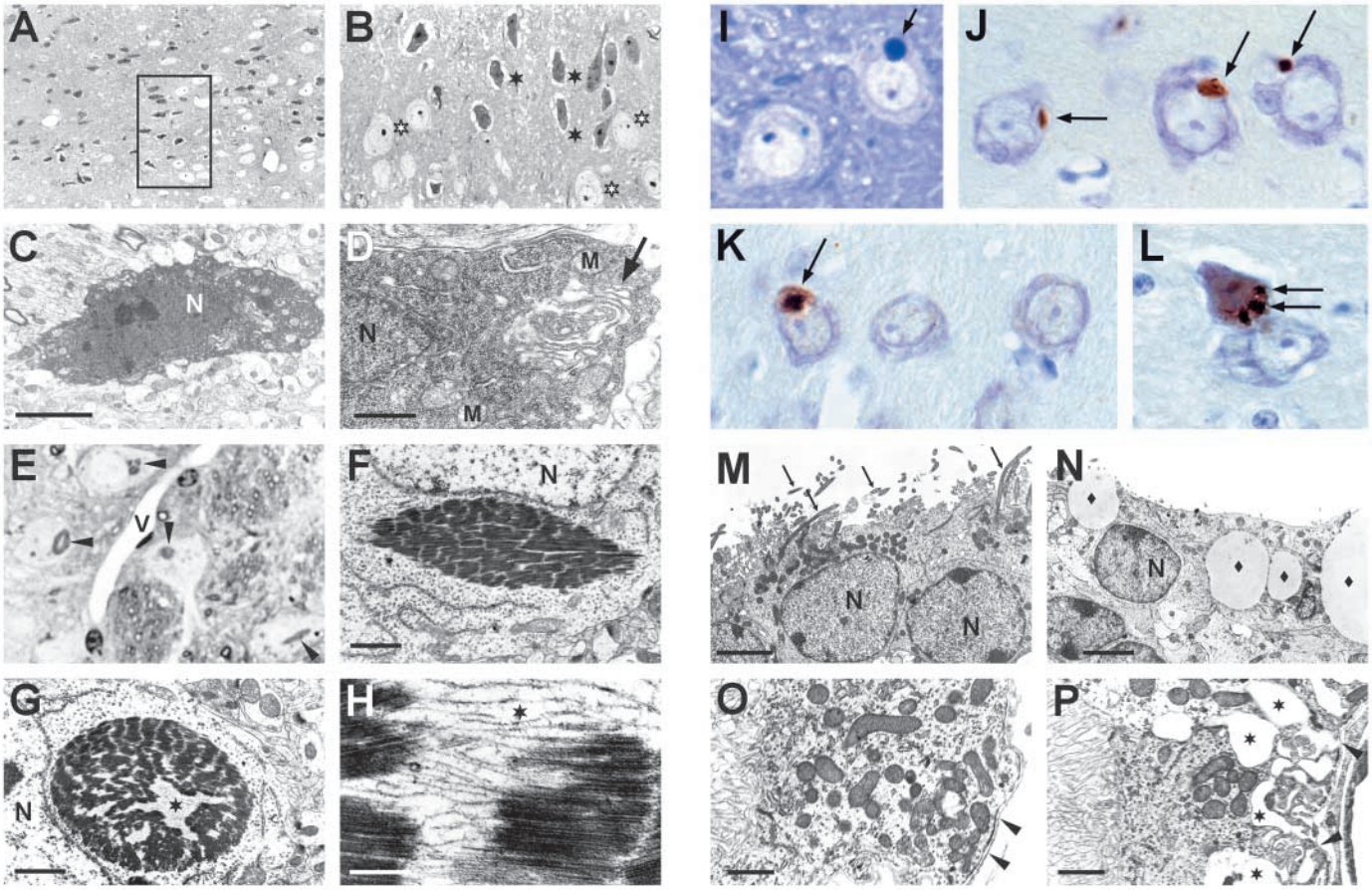

Fig. 7. Degeneration and pathological cytoplasmic aggregates in mutant neurones, and abnormality of mutant ependyma and choroid plexi. (A-D) Degenerating neurones. (A) Semithin section stained with Toluidine Blue showing abundant shrunken and hyperchromic degenerating cells in the thalamus (centromedian nucleus) of mutant mice. The same cell abnormalities were observed in dorsal striatum and septum (not shown). (B) Detail of A. White asterisks indicate healthy neurones; black asterisks indicate shrunken and hyperchromatic pathological neurones. (C,D) Electron microscopy of hyperchromatic cell. Note the high electron density of the cytoplasm and nucleus, the cytoplasmic and nuclear membrane irregularities, and the dilated Golgi cisternae (indicated by arrows). N, nucleus; M, mitochondria. Scale bars: 2.5 μm in C; 0.5 μm in D. (E-L) Intraneuronal aggregates. (E) Semithin section stained with Toluidine Blue showing abundant intraneuronal perinuclear aggregates in the thalamus (ventrobasal nuclei) of mutant mice. The inclusions in the cells at the far left and lower right are similar to those shown by electron microscopy in F and G, respectively. Arrowheads point to aggregates. V, blood vessel. (F,G,H) Electron microscopy of aggregates. Asterisks indicate the central clearer region, seen at higher magnification in H. The inclusions show abundant filamentous content, with a filament diameter of 9-10 μm. Scale bars: 1 μm in F,G; 0.2 μm in H. (I) Semithin section showing inclusion-containing and normal neurones, stained with Toluidine Blue. Arrow indicates aggregate showing typical perinuclear location. (J-L) Immunohistochemistry (on paraffin sections) with anti-neurofilament (SMI 32; J) and anti-ubiquitin (K,L) antibodies. Positive staining was also observed with SMI 31 (anti-phosphorylated neurofilaments) antibody (not shown). Arrows indicate immunostained intraneuronal aggregates. Note the normal morphology of the aggregate-containing neurones in J and K, and the pathological morphology of the hyperchromatic aggregate-containing neurone in L (see text). In K, note the weaker immunostaining (light brown) in the cell on the right. (M,N) Wild-type (M) and mutant (N) ependyma. Black diamond indicates lipidic inclusions; arrows indicate cilia. N, nucleus. (O,P) Wild-type (O) and mutant (P) choroid plexi. Left, apical microvilli; right, basal membrane, with numerous infoldings (asterisk) in the mutant. Arrowheads point to basal membrane.

cells were decreased in mutant mice, by nearly 80% (Fig. 8F). These results demonstrate a profound defect in lateral ventricle neurogenesis, as was also seen in the hippocampus (see above).

In contrast to the BrdU incorporation defects observed postnatally, no significant differences between normal and mutant were observed when labelling was done in the embryo for a single day (between E12.5 and E16.5) and analysis was performed 24 hours later (to detect newly born neural cells) or a month later (to detect neurones labelled during their terminal division). It is conceivable that embryonic cells might be less dependent than adult cells on *Sox2* levels, possibly because of Sox family gene redundancy, or because of higher normal expression of *Sox2* in these cells.

Discussion

Sox2 is a transcription factor necessary for the proliferation/maintenance of at least one type of stem cell, the epiblast stem cell (Avilion et al., 2003). In this work, we have examined the expression and function of mouse *Sox2* in brain neural cells. We find that *Sox2* is expressed in neural stem/precursor cells

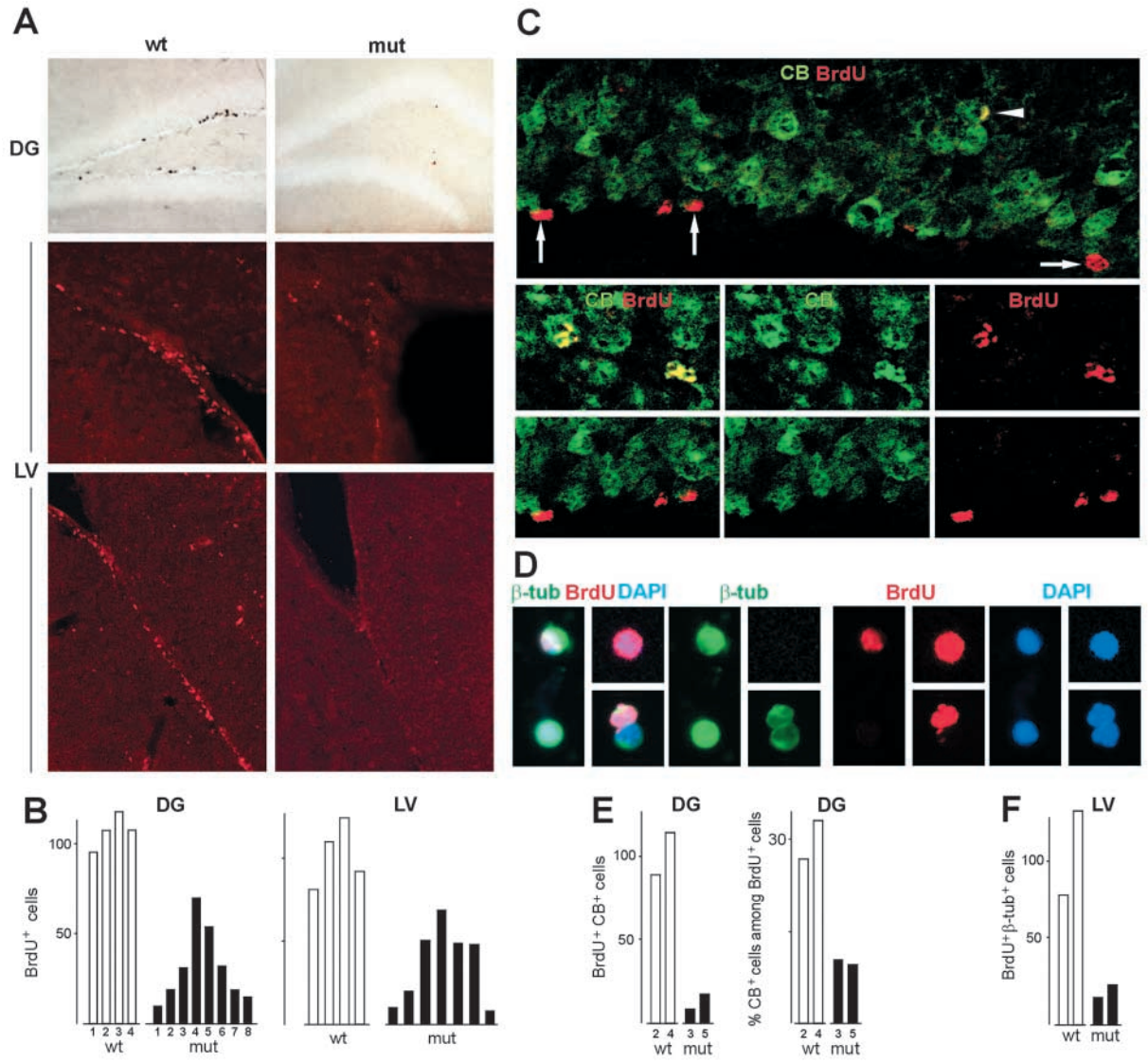

Fig. 8. Reduced cell proliferation and impaired neurogenesis in adult mutant neurogenic regions. (A) Decreased BrdU labelling in mutant (right) versus wild-type (left) hippocampus dentate gyrus (DG, top) and lateral ventricle (LV, bottom). BrdU immunoreactivity was revealed by diaminobenzydine (DAB) staining (brown) in the hippocampus, and by rhodamine fluorescence (red) in the lateral ventricle. In the lateral ventricle, the upper panel shows the top lateral corner, and the lower panel shows the ventrolateral wall of the ventricle. (B) Quantitation of BrdU labelling. The average number of BrdU-positive cells in wild-type mice was set equal to 100. Each bar corresponds to the total number of BrdU-positive nuclei in the lateral ventricle walls (LV, left) or in the hippocampus dentate gyrus germinative layer (DG, right) of an individual mouse (white bars, wild type; black bars, mutants). (C**)** Double fluorescence immunohistochemistry for BrdU (red) and calbindin (CB, green, marking mature granule neurones) on hippocampus dentate gyrus (confocal microscopy). Mice were treated with BrdU for 12 days. BrdU/CB double-positive cells (yellow) are newborn neurones still retaining the label (BrdU) of a recently divided precursor. White arrows indicate BrdU-positive, CB-negative precursors at the base of the granule cell layer; the white arrowhead indicates a BrdU/CB double-positive cell within the granule cell layer (yellow). Quantitative assessment is shown in E. (D) Double fluorescence immunocytochemistry for BrdU (red) and β-tubulin (green, marking neuroblasts) on dissociated cells from the periventricular region of the lateral ventricle of mice treated with BrdU for 7 days (blue, DAPI nuclear staining). Note that β-tubulin staining is cytoplasmic. An example of five different cells, stained with all three labels and viewed as a merged image, is shown on the left (β-tub, BrdU, DAPI). The corresponding single fluorescence images are shown in the panels to the right. Double-positivity for BrdU and β-tubulin results in a pink nuclear image (due to overlap of the red BrdU staining with the blue DAPI) partially surrounded by a blue-green halo (top left cell). Single positivity for BrdU results in a pink image (top right cell), whereas single positivity for β-tubulin results in a blue-green colour (bottom left cell). At the bottom right, note the doublet consisting of a doubly positive cell and a single β-tubulin-positive cell. (E) Quantitation of BrdU/CB double-positive cells (left histogram), and of the proportion of CB-positive cells among BrdU-positive cells, in the dentate gyrus of wild-type (white bars) and mutant (black bars) mice (see C). The average number of BrdU/CB double-positive cells counted in wild-type mice was 71 (5 sections per mouse counted), and was set equal to 100 (left histogram). The average proportion of CB-positive cells among BrdU-positive cells was 31% in wild-type mice. Each bar corresponds to one mouse, identified by numbers on the *x* axis (see also panel B). (F) Quantitation of BrdU/β-tubulin double-positive cells in dissociated periventricular cells of the lateral ventricle from wild-type and mutant mice (see panel D). The average value for wild-type mice (corresponding to 60 double-positive cells/four chambered wells counted) was set equal to 100.

of adult mouse, and is required for their proliferation/maintenance. In addition to neural proliferation defects, adult brains of *Sox2* mutants show loss of thalamo-striatal parenchyma, cell degeneration and neurological abnormalities.

Reduction of *Sox2* expression in *Sox2*$^{\beta\text{-geo}/\Delta\text{ENH}}$ compound heterozygotes is sufficient to cause brain defects

We have combined a null mutation of *Sox2* (*Sox2*$^{\beta\text{-geo}}$) with a regulatory ('knockdown') mutation (*Sox2*$^{\Delta\text{ENH}}$), obtained by deleting a neural-specific enhancer (Zappone et al., 2000) from the *Sox2* locus. Although the latter deletion decreases *Sox2* expression, it does not abolish it (Zappone et al., 2000) (see also Figs S1, S2 at http://dev.biologists.org/supplemental/).

Neither the heterozygous null mutant (*Sox2*$^{\beta\text{-geo}/+}$), nor the homozygous knockdown mutants (*Sox2*$^{\Delta\text{ENH}/\Delta\text{ENH}}$) show any pathology, with the exception of some mild ventricle enlargement in occasional heterozygous null (*Sox2*$^{\beta\text{-geo}/+}$) mice. Significantly, this suggests that the observed phenotype is critically sensitive to thresholds effects; in fact, a pathological phenotype is observed in *Sox2*$^{\beta\text{-geo}/\Delta\text{ENH}}$ compound heterozygotes, at a level of expression of *Sox2* of 25-30% (relative to wild type), moderately below the level expected for the unaffected *Sox2*$^{\beta\text{-geo}/+}$ null heterozygote. This effect resembles that observed with combinations of different knockdown alleles of the *Fgf8* gene (Meyers et al., 1998). Importantly, it is unlikely that the regulatory *Sox2*$^{\Delta\text{ENH}}$ mutation causes its effects through interference with adjacent genes, as no pathological effects are observed in mice homozygous for this mutation.

Thalamo-striatal defects and neurodegeneration in adult *Sox2* mutants

A major defect of *Sox2*$^{\beta\text{-geo}/\Delta\text{ENH}}$ mutant mice is the loss of thalamo-striatal parenchyma with ventricle enlargement. In murine models of Huntington's and Alzheimer's disease, parenchymal loss with secondary ventricle enlargement represents the consequence of primary neurodegeneration (Capsoni et al., 2000; Yamamoto et al., 2000; Mantamadiotis et al., 2002). The correlation between the expression of *Sox2* (in the late foetal and in the adult periods) in the differentiated parenchyma of thalamus and striatum (Figs 2, 3), and the tissue loss (Fig. 6) with abundant neurodegeneration (Fig. 7) in these same areas in compound *Sox2*$^{\beta\text{-geo}/\Delta\text{ENH}}$ mutants, implies an important functional role of *Sox2* for adult neurones.

An additional unexpected observation is the presence of intracellular inclusions in neurones, close to (and occasionally within) the degenerated cells (Fig. 7). Protein inclusions in neurodegenerative diseases are caused by the aggregation of potentially toxic misfolded proteins, and may represent an 'attempt' to clear the cell of harmful proteins through, for example, ubiquitination (Bucciantini et al., 2002; Taylor et al., 2002; Zoghbi and Botas, 2002). In inherited human neurodegenerative disorders, aggregates are often the result of mutations in a gene

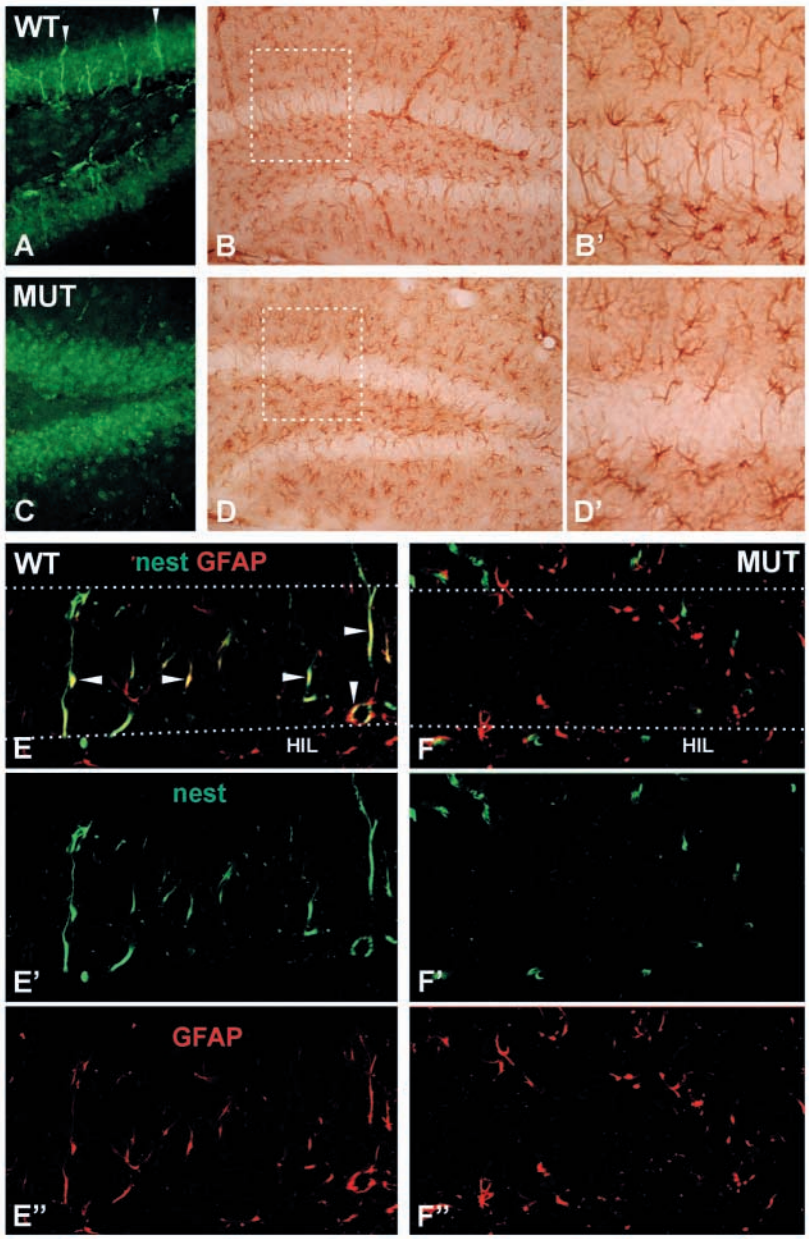

Fig. 9. Nestin- and GFAP-positive early precursors are severely reduced in mutant hippocampus. (A,C) Immunofluorescence detection of radially oriented nestin-expressing cells (bright green; white arrowheads) in wild-type (A) and mutant (C) hippocampus. (B,B′,D,D′) Immunohistochemical detection (DAB, brown) of GFAP-expressing cells in wild-type (B) and mutant (D) hippocampus. Note, in the enlargement of the boxed areas (B′,D′), the severe reduction of GFAP-positive radially oriented cells within the dentate gyrus. (E,F) Double immunofluorescence detection of nestin (E,E′,F,F′; green)/GFAP (E,E″,F,F″; red) double-positive precursor cells in the hippocampus dentate gyrus of wild-type (E) and mutant (F) mice. Double-positive cells are indicated by white arrowheads. The dotted lines define the dentate gyrus region. HIL, hilus.

encoding a structural protein found in the aggregates themselves (e.g. alpha-synuclein, huntingtin), or of an enzyme (e.g. presenilin) involved in protein processing (Taylor et al., 2002; Zoghbi and Botas, 2002).

However, in the majority of 'common' multifactorial degenerations, aggregates may represent a progressive, age-related response to 'environmental' (i.e. metabolic, toxic) factors. Few genetic modifiers of this response have been identified (Zoghbi and Botas, 2002). Neurofilament-rich aggregates ultrastructurally very similar to those described here were reported in the thalamus of mice with thiamine-deficient encephalopathy (Aikawa et al., 1983), and of a small proportion of aging mice (Fraser, 1969). The development after birth of large numbers of inclusion-containing neurones in mutant but not control mice, at a relatively young age, indicates that *Sox2* deficiency can represent a major genetic contribution to this pathology. In conclusion, the presence, in mutants, of inclusion-containing neurones and, in particular, of degenerated cells (see above), shows that *Sox2* is required for the maintenance of vital functions of neurones. *Sox2*, being a transcription factor, might, directly or indirectly, affect the activity of genes encoding chaperons, proteolytic enzymes, and so on, involved in general mechanisms of neurone protection. It will be interesting to evaluate whether *Sox2* deficiency increases the severity of other mutations causing neurodegeneration (Zoghbi and Botas, 2002), by breeding to appropriate strains.

The expression of *Sox2* in the ependyma, together with the lipidic inclusions and ciliary loss, raises the possibility that malfunction of these cells may also contribute to the development of hydrocephalic features. Hereditary hydrocephalus is observed in humans with Karthagener's syndrome, a primary ciliary dyskinesia. It is also observed in the mouse knock-out model of the dynein gene *Mdnah5* (*Dnahc5* – Mouse Genome Informatics), which is essential for ciliary mobility (Ibanez-Tallon et al., 2002), or of the *Isg15* (*Glp2* – Mouse Genome Informatics) gene, which encodes an ependymal ubiquitin ligase (Ritchie et al., 2002). However, we note that in *Sox2* mutants the cortex, which in primary hydrocephalus is often very thin because of cerebrospinal fluid pressure (Lindeman et al., 1998; Ibanez-Tallon et al., 2002; Ritchie et al., 2002), is comparatively unaffected and does not show neuronal pathology. Conversely, thalamo-striatal neuronal pathology with intraneuronal inclusions is not described in primary hydrocephalus with ventricle enlargement that is even more pronounced than that seen in *Sox2* mutants (Lindeman et al., 1998; Ibanez-Tallon et al., 2002; Ritchie et al., 2002; Blackshear et al., 2003).

The regions affected by neuropathology are part of the nigro-striatal-cortico-thalamic circuitry, which controls motor behaviour and requires dopamine as a crucial neurotransmitter (Carlsson, 2001). This makes their lesion a plausible reason for the functional defects observed. Some of these defects, such as circling, have been likened to those observed in humans with Parkinson's disease (Kim et al., 2002). Dopaminergic neurones of the substantia nigra, whose lesion causes Parkinson's disease in humans, do not show gross abnormalities or important reduction of TH immunoreactivity in our mutants (not shown). It should be considered that the vulnerability of these neurones to damage (and aggregate formation) appears to be extremely reduced in mice versus humans (Lee et al., 2002). Thus, motor dysfunction in mouse models, including the *Sox2* mutant, might be due to defects located elsewhere in the basal ganglia-thalamocortical circuitry (Carlsson, 2001; Wang et al., 2002). Interestingly, in preliminary experiments we found altered GABA immunoreactivity in the same thalamic nuclei that the neuropathology is observed in (S.D.B. and S.K.N., unpublished).

Sox2 is expressed in neural precursor cells

In the adult brain, neural stem cells divide at a low rate, both renewing themselves and generating neural precursors. Virtually all newly divided cells (i.e. $BrdU^+$ cells) express *Sox2* in both the subventricular region and hippocampus subgranular zone (Fig. 4). These results suggest that *Sox2* is expressed in the majority, if not all, of the neural precursor cells. A number of observations suggest that *Sox2* might be expressed in stem cells as well. (1) Within the subventricular region, a proportion of *Sox2*-positive cells also express GFAP; GFAP-positive cells (B cells) within this location have been proposed to include stem cells (Doetsch et al., 1999), and their morphology (Doetsch et al., 1999; Doetsch, 2003) strikingly resembles that observed by us for SOX2/GFAP double-positive cells (see Fig. 4D). (2) In the hippocampus subgranular zone, GFAP/SOX2 double-positive cells, characteristically extending radial processes into the dentate gyrus, are detected (Fig. 4H); again, the location and morphology of these cells are strongly reminiscent of GFAP-positive (Seri et al., 2001) and GFAP/nestin-positive (Fukuda et al., 2003) cells thought to include the in vivo hippocampal primary precursors (Seri et al., 2001; Fukuda et al., 2003; Doetsch, 2003). (3) In in vitro culture, $Sox2^{\beta\text{-geo}}$-expressing cells show functional properties of neural stem cells (self renewal, multipotency) throughout extensive propagation in the presence of G418 (implying continued *Sox2* expression in these cells).

In *Sox2* mutants, neural precursor proliferation and neurogenesis are affected

In adult *Sox2* mutants, BrdU labelling in the subventricular zone and hippocampus is strongly decreased (Fig. 8A,B). This might be due either to loss of stem cells/precursors, or to a decreased ability to proliferate in response to physiological stimuli. Our results suggest that, in the hippocampus, both the number of stem/precursor cells, and the ability of their progeny to differentiate into neurones, is decreased (Figs 8, 9). In fact, GFAP/nestin double-positive cells, which represent the earliest precursors to neurones in the dentate gyrus (Fukuda et al., 2003), are dramatically decreased in *Sox2* mutants (Fig. 9). This is in agreement with the presence of SOX2 in GFAP-positive subventricular cells (see above), and suggests that *Sox2* is cell-autonomously requested for the maintenance of these cells. In addition, the proportion of calbindin-positive cells (i.e. neurones) within BrdU-positive cells is decreased (Fig. 8E), indicating that newly generated precursors may either die or fail to differentiate properly. A similar result is obtained in the subventricular zone; here, the number of BrdU/β-tubulin III double-positive (i.e. recently generated early neuronal) cells is strongly decreased (Fig. 8F). Thus, both in the hippocampus and subventricular zone, neurogenesis is strongly affected.

It has been speculated that neuronal cell replacement by endogenous precursors in adults, following chronic

neurodegeneration, might slow down the course of the disease (Kruger and Morrison, 2002). If this were the case, the decreased neurogenesis in *Sox2* mutants might contribute to the severity of the phenotype.

Recent experiments in chicken using electroporation of a Sox-dominant negative construct (affecting *Sox1*, *Sox2* and *Sox3* activities) suggest that at least one member of the SOX family is necessary to prevent premature commitment to differentiation; alternatively, a single Sox gene expressed ectopically prevents neural differentiation (Graham et al., 2003; Bylund et al., 2003). Our experiments are consistent with a role of Sox family members in the maintenance of functional properties of neural precursor cells (Graham et al., 2003; Bylund et al., 2003). However, the situation may be more complex. We show that adult neural precursors, in mouse, are specifically sensitive to *Sox2* gene dosage, even in the presence of normal *Sox1* and *Sox3* genes. It is possible that the subset of neural precursors affected by *Sox2* deficiency do not co-express *Sox1* and/or *Sox3* together with *Sox2*; alternatively, *Sox2* might play specific functions within these cells that cannot be complemented by *Sox1* and *Sox3*. Furthermore, *Sox2* may also affect cell survival or differentiation even downstream of the precursor stages, as shown by the requirement for *Sox2* in neurone generation (see above, and Fig. 8), and in preventing the death or degeneration of some differentiated neurones (Fig. 7). As important neural cell and brain alterations are detected in $Sox2^{\beta\text{-geo}/\Delta ENH}$ compound heterozygotes retaining significant amounts of *Sox2*, it will be important to assess the effect of the complete ablation of *Sox2* expression in different types of neural cells using a conditional *Sox2* knock-out strategy.

Recently, it was shown (Fantes et al., 2003) that heterozygous *Sox2* truncating-point mutations in humans are associated with anophtalmia, and with variable extraocular defects, including seizures, microcephaly and motor abnormalities. The ocular phenotype of our mutant mice is presently being investigated. However, these observations in humans, taken together with our findings, suggest that it might be worth looking for *Sox2* defects in a wider range of inherited human neurological diseases.

We thank Gianni Dehò for the suggestion and gift of CMB-*E. coli*; Ron McKay for the anti-nestin antiserum; Letizia Longo for help with ES cell karyotyping; Stefano Mantero for advice on in situs; Giovanni Bertoni, Tino Vidal Aroca, Laura Spinardi and Laura Vitellarozuccarello for help with densitometric analysis and confocal imaging; and Heather Cameron, Roger Davis, Fabrizio Tagliavini, Giorgio Giaccone, Silvana Franceschetti, Suzanne Donini, Roberto Taramelli, Antonio Simeone, Sally Temple, Alexandra Capela and Raja Kittappa for precious advice and discussion on the many scientific and technical issues we encountered during this work. We also thank Daniela Santoni for her expert mouse care, and Mario Azzini for excellent photographic assistance. This work was supported by grants from Telethon (D.127), the EEC (QLG3-CT-01141C00) and MIUR-COFIN to S.K.N., and by a FIRB grant to E. Cattaneo.

References

Avilion, A. A., Nicolis, S. K., Pevny, L. H., Perez, L., Vivian, N. and Lovell-Badge, R. (2003). Multipotent cell lineages in early mouse development depend on SOX2 function. *Genes Dev.* **17**, 126-140.

Aikawa, H., Suzuki, K. and Iwasaki, Y. (1983). Ultrastructural observation on the thalamic neuronal inclusions in young mice. *Acta Neuropathol.* **59**, 316-318.

Blackshear, P. J., Graves, J. P., Stumpo, D. J., Cobos, I., Rubenstein, J. L. and Zeldin, D. C. (2003). Graded phenotypic response to partial and complete deficiency of a brain-specific transcript variant of the winged helix transcription factor RFX4. *Development* **130**, 4539-4552.

Braida, D., Pozzi, M. and Sala, M. (2000). CP 55,940 protects against ischemia-induced electroencephalographic flattening and hyperlocomotion in Mongolian gerbils. *Neurosci. Lett.* **296**, 69-72.

Bucciantini, M., Giannoni, E., Chiti, F., Baroni, F., Formigli, L., Zurdo, J., Taddei, N., Ramponi, G., Dobson, C. M. and Stefani, M. (2002). Inherent toxicity of aggregates implies a common mechanism for protein misfolding diseases. *Nature* **416**, 507-511.

Bylund, M., Andersson, E., Novitch, B. G. and Miuhr, J. (2003). Vertebrate neurogenesis is counteracted by Sox1-3 activity. *Nat. Neurosci.* **11**, 1162-1168.

Capela, A. and Temple, S. (2002). LeX/ssea-1 is expressed by adult mouse CNS stem cells, identifying them as nonependymal. *Neuron* **35**, 865-875.

Capsoni, S., Ugolini, G., Comparini, A., Ruberti, F., Berardi, N. and Cattaneo, A. (2000). Alzheimer-like neurodegeneration in aged antinerve growth factor transgenic mice. *Proc. Natl. Acad. Sci. USA* **97**, 6826-6831.

Carlsson, A. (2001). A paradigm shift in brain research. *Science* **294**, 1021-1024.

Doetsch, F., Garcìa-Verduga, J. M. and Alvarez-Buylla A. (1997). Cellular composition and three-dimensional organization of the subventricular germinal zone in the adult mammalian brain. *J. Neurosci.* **17**, 5046-5061.

Doetsch, F., Caille, I., Lim, D. A., Garcia-Verdugo, J. M. and Alvarez-Buylla, A. (1999). Subventricular zone astrocytes are neural stem cells in the adult mammalian brain. *Cell* **97**, 703-716.

Doetsch, F. (2003). The glial identity of neural stem cells. *Nat. Neurosci.* **6**, 1127-1134.

Fantes, J., Ragge, N. K., Lynch, S. A., McGill, N. I., Collin, J. R., Howard-Peebles, P. N., Hayward, C., Vivian, A. J., Williamson, K., van Heyningen, V. and FitzPatrick, D. R. (2003). Mutations in SOX2 cause anophthalmia. *Nat. Genet.* **33**, 461-463.

Fraser, H. (1969). Eosinophilic bodies in some neurones in the thalamus of ageing mice. *J. Pathol.* **98**, 201-204.

Fukuda, S., Kato, F., Tozuka, Y., Yamaguchi, M., Miyamoto, Y. and Hisatune, T. (2003). Two distinct subpopulations of nestin-positive cells in adult mouse dentate gyrus. *J. Neurosci.* **23**, 9357-9366.

Gage, F. H. (2000). Mammalian neural stem cells. *Science* **287**, 1433-1438.

Gould, E., Beylin, A., Tanapat, P., Reeves, A. and Shors, T. J. (1999). Learning enhances adult neurogenesis in the hippocampal formation. *Nat. Neurosci.* **2**, 260-265.

Graham, V., Khudyakov, J., Ellis, P. and Pevny, L. (2003). SOX2 functions to maintain neural progenitor identity. *Neuron* **39**, 749-765.

Gubbay, J., Collignon, J., Koopman, P., Capel, B., Economou, A., Münsterberg, A., Vivian, N., Goodfellow, P. and Lovell-Badge, R. (1990). A gene mapping to the sex-determining region of the mouse Y chromosome is a member of a novel family of embryonically expressed genes. *Nature* **346**, 245-250.

Hodgson, J. G., Agopyan, N., Gutekunst, C. A., Leavitt, B. R., LePiane, F., Singaraja, R., Smith, D. J., Bissada, N., McCutcheon, K., Nasir, J., Jamot, L., Li, X. J., Stevens, M. E., Rosemond, E., Roder, J. C., Phillips, A. G., Rubin, E. M., Hersch, S. M. and Hayden, M. R. (1999). A YAC mouse model for Huntington's disease with full-length mutant huntingtin, cytoplasmic toxicity, and selective striatal neurodegeneration. *Neuron* **23**, 181-192.

Ibanez-Tallon, I., Gorokhova, S. and Heintz, N. (2002). Loss of function of axonemal dynein Mdnah5 causes primary ciliary dyskinesia and hydrocephalus. *Hum. Mol. Genet.* **11**, 715-721.

Johansson, C. B., Momma, S., Clarke, D. L., Risling, M., Lendahl, U. and Frisen, J. (1999). Identification of a neural stem cell in the adult mammalian central nervous system. *Cell* **96**, 25-34.

Kamachi, Y., Uchikawa, M. and Kondoh, H. (2000). Pairing SOX off, with partners in the regulation of embryonic development. *Trends Genet.* **16**, 182-187.

Kempermann, G., Kuhn, H. G. and Gage, F. H. (1997). More hippocampal neurons in adult mice leaving in an enriched environment. *Nature* **386**, 493-495.

Kim, J. H., Auerbach, J. M., Rodriguez-Gomez, J. A., Velasco, I., Gavin, D., Lumelsky, N., Lee, S. H., Nguyen, J., Sanchez-Pernaute, R., Bankiewicz, K. and McKay, R. (2002). Dopamine neurons derived from

embryonic stem cells function in an animal model of Parkinson's disease. *Nature* **418**, 50-56.

Kishi, M., Mizuseki, K., Sasai, N., Yamazaki, H., Shiota, K., Nakanishi, S. and Sasai, Y. (2000). Requirement of Sox2-mediated signaling for differentiation of early Xenopus neuroectoderm. *Development* **127**, 791-800.

Kruger, G. M. and Morrison, S. J. (2002). Brain repair by endogenous progenitors. *Cell* **110**, 399-402.

Lee, M. K., Stirling, W., Xu, Y., Xu, X., Qui, D., Mandir, A. S., Dawson, T. M., Copeland, N. G., Jenkins, N. A. and Price, D. L. (2002). Human alpha-synuclein-harboring familial Parkinson's disease-linked Ala-53 → Thr mutation causes neurodegenerative disease with alpha-synuclein aggregation in transgenic mice. *Proc. Natl. Acad. Sci. USA* **99**, 8968-8973.

Lindeman, G. J., Dagnino, L., Gaubatz, S., Xu, Y., Bronson, R. T., Warren, H. B. and Livingston, D. M. (1998). A specific, nonproliferative role for E2F-5 in choroid plexus function revealed by gene targeting. *Genes Dev.* **12**, 1092-1098.

McDevitt, M. A., Shivdasani, R. A., Fujiwara, Y., Yang, H. and Orkin, S. H. (1997). A 'knockdown' mutation created by cis-element gene targeting reveals the dependence of erythroid cell maturation on the level of transcription factor GATA-1. *Proc. Natl. Acad. Sci. USA* **94**, 6781-6785.

McKay, R. (1997). Stem cells in the central nervous system. *Science* **276**, 66-71.

Mangiarini, L., Sathasivam, K., Seller, M., Cozens, B., Harper, A., Hetherington, C., Lawton, M., Trottier, Y., Lehrach, H., Davies, S. W. and Bates, G. P. (1996). Exon 1 of the HD gene with an expanded CAG repeat is sufficient to cause a progressive neurological phenotype in transgenic mice. *Cell* **87**, 493-506.

Mantamadiotis, T., Lemberger, T., Bleckmann, S. C., Kern, H., Kretz, O., Martin, V. A., Tronche, F., Kellendonk, C., Gau, D., Kapfhammer, J., Otto, C., Schmid, W. and Schutz, G. (2002). Disruption of CREB function in brain leads to neurodegeneration. *Nat. Genet.* **31**, 47-54.

Meyers, E. N., Lewandoski, M. and Martin, G. R. (1998). An Fgf8 mutant allelic series generated by Cre- and Flp-mediated recombination. *Nat. Genet.* **18**, 136-141.

Ritchie, K. J., Malakhov, M. P., Hetherington, C. J., Zhou, L., Little, M. T., Malakhova, O. A., Sipe, J. C., Orkin, S. H. and Zhang, D. E. (2002). Dysregulation of protein modification by ISG15 results in brain cell injury. *Genes Dev.* **16**, 2207-2212.

Schwenk, F., Baron, U. and Rajewsky, K. (1995). A cre-transgenic mouse strain for the ubiquitous deletion of loxP-flanked gene segments including deletion in germ cells. *Nucleic Acids Res.* **23**, 5080-5081.

Seri, B., Garcia-Verdugo, J. M., McEwen, B. S. and Alvarez-Buylla, A. (2001). Astrocytes give rise to new neurons in the adult mammalian hippocampus. *J. Neurosci.* **21**, 7153-7160.

Tanemura, K., Murayama, M., Akagi, T., Hashikawa, T., Tominaga, T., Ichikawa, M., Yamaguchi, H. and Takashima, A. (2002). Neurodegeneration with tau accumulation in a transgenic mouse expressing V337M human tau. *J. Neurosci.* **22**, 133-141.

Taylor, J. P., Hardy, J. and Fischbeck, K. H. (2002). Toxic proteins in neurodegenerative disease. *Science* **296**, 1991-1995.

Temple, S. (2001). The development of neural stem cells. *Nature* **414**, 112-117.

Temple, S. and Alvarez-Buylla, A. (1999). Stem cells in the adult mammalian central nervous system. *Curr. Opin. Neurobiol.* **9**, 135-141.

Turmaine, M., Raza, A., Mahal, A., Mangiarini, L., Bates, G. P. and Davies, S. W. (2000). Nonapoptotic neurodegeneration in a transgenic mouse model of Huntington's disease. *Proc. Natl. Acad. Sci. USA* **97**, 8093-8097.

Uwanogho, D., Rex, M., Cartwright, E. J., Pearl, G., Healy, C., Scotting, P. J. and Sharpe, P. T. (1995). Embryonic expression of the chicken Sox2, Sox3 and Sox11 genes suggests an interactive role in neuronal development. *Mech. Dev.* **49**, 23-36.

Vezzani, A., Moneta, D., Conti, M., Richichi, C., Ravizza, T., De Luigi, A., De Simoni, M. G., Sperk, Andell-Jonsson, S., Lundkvist, J., Iverfeldt, K. and Bartfai, T. (2000). Powerful anticonvulsant action of IL-1 receptor antagonist upon intracerebral injection and astrocytic overexpression in mice. *Proc. Natl. Acad. Sci. USA*, **97**, 115-134.

Wang, Q., Bardgett, M. E., Wong, M., Wozniak, D. F., Lou, J., McNeil, B. D., Chen, C., Nardi, A., Reid, D. C., Yamada, K. and Ornitz, D. M. (2002). Ataxia and paroxysmal dyskinesia in mice lacking axonally transported FGF14. *Neuron* **35**, 25-38.

Wilkinson, D. G. (1998). *In Situ Hybridization, A Practical Approach*. Oxford, Oxford University Press.

Wood, H. B. and Episkopou, V. (1999). Comparative expression of the mouse Sox1, Sox2 and Sox3 genes from pre- gastrulation to early somite stages. *Mech. Dev.* **86**, 197-201.

Yamamoto, A., Lucas, J. J. and Hen, R. (2000). Reversal of neuropathology and motor dysfunction in a conditional model of Huntington's disease. *Cell* **101**, 57-66.

Zappone, M. V., Galli, R., Catena, R., Meani, N., De Biasi, S., Mattei, E., Tiveron, C., Vescovi, A. L., Lovell-Badge, R., Ottolenghi, S. and Nicolis, S. K. (2000). Sox2 regulatory sequences direct expression of a β-geo transgene to telencephalic neural stem cells and precursors of the mouse embryo, revealing regionalization of gene expression in CNS stem cells. *Development* **127**, 2367-2382.

Zoghbi, H. Y. and Botas, J. (2002). Mouse and fly models of neurodegeneration. *Trends Genet.* **18**, 463-471.